ERASMUS MUNDUS MASTER OF MECHANICAL ENGINEERING

MEMOIRE-THESIS

Weerachai Chaiworapuek

The Engineering Investigation of the Water Flow past the Butterfly Valve

June 2007

INSTITUT NATIONAL DES SCIENCES APPLIQUEES DE LYON - FRANCE
ESCOLA TÈCNICA SUPERIOR D'ENGINYERIA INDUSTRIAL DE BARCELONA, UNIVERSITAT POLITÈCNICA DE CATALUNYA - ESPAGNE
THE COLLEGE OF THE HOLY AND UNDIVIDED TRINITY OF QUEEN ELIZABETH NEAR DUBLIN - IRLANDE

Abstract

This paper presents a numerical simulation of flow past the butterfly valve in static and dynamic analysis using commercial fluid dynamics software FLUENT. In static analysis, the positions of the disk were set to be $0°$ (completely opened), $30°$, $45°$, $60°$ and $75°$ under 1, 2 and 3 m/s water speed. The values of angular velocity were set to be 0.039 and 1.57 rad/s under 1 m/s water speed in dynamic analysis. The study focuses on the investigation of the characteristic of loss coefficient and torque behavior of the 150 mm and 300 mm butterfly valve. From the results obtained, it was found that the loss coefficient and torque values increased when the disk angle was increased. By increasing the water speed, the loss coefficient remained constant while torque value increased. In dynamic analysis of both angular speeds, the maximum torque occurred around $70° - 80°$ in closing turn and $100° - 110°$ in opening turn. The experiment was also carried out to verify the numerical results. By comparing between the experimental and numerical method, it was found that the loss coefficient and torque value could be determined responsibly. The acceptable comparisons were seen.

Acknowledgements

Firstly, I'd like to thank for Erasmus Mundus programme for a great opportunity to study in Ireland and France. I also would like to thank for Professor Jean-Yves Champagne and M. El Hajem Mahmoud of the Génie Mécanique Conception, INSA-Lyon, France for encouragement, suggestion and everything throughout this project. Thank for Bertrand Voisin and Didier Desseux for helps in the experimental part of this project. And also thank for Professor Henry Rice of the department of mechanical and manufacturing engineering, Trinity College, Dublin, Ireland for everything in the first year.

I'd like to thank for friends ; Venu Goru, Zhou Ze, Cui Yu, Rafael Sanches and Shekhar Tyagi for everything during this two years. It is my unforgettable memory.

Finally, I would like to thank for Kitti and Sanga Chaiworapuek, my parents ; Noppanan Chaiworapuek my brother ; especially, Jeab for all of encouragements.

List of Figures

List of Figures(continued)

List of Figures(continued)

List of Figures(continued)

List of Tables

Contents

Chapter 1 Introduction

The opened-closed controller or safety unit for fluid-flow in piping system is a necessary element in every piping configuration. One of the most well-known is butterfly valve. The butterfly valve has 3 main components consisting of the body, the shaft and the valve disk. It is commonly set up into the system to induce the flow as well as to be a safety device. Not only its low cost but also its simple mechanical assembly that makes the butterfly valve to be useful over any other valves. Butterfly valve also provides the large flow capacity at the completely open position. Moreover when compared to various valve designs of comparable size, butterfly valve are also advantageous.

The main standard variables of butterfly valve, considering for classification are the loss coefficient and the hydrodynamic torque. The loss coefficient is individual value in each type of valve. This value that is caused by flow through a valve becomes significant parameter for unique valve. Normally, the primary objective of butterfly valve is to regulate the flow rate. This will be accomplished by changing the geometry of the butterfly valve. For example: opening or closing the valve will change the flow characteristics inside the pipe. And for one butterfly valve, the flow field characteristics will also behave differently in different angle of attack of valve disk. However the loss behavior of any valve geometry can be proposed by the loss coefficient.

Another parameter is torque which is obviously used to rotate the position of the valve disk. The value of torque strongly depends on 2 factors consisting of hydrodynamic torque and friction torque. Changing the angle of butterfly valve disk and flow capacity as well as the size of water pipe can induce the flow which influent the pressure profile on the disk surface and the resulting hydrodynamic torque. Therefore, to investigate the hydrodynamic torque characteristic, the basic parameters such as volume flow rate, size of pipe and position of disk need to be set in different cases.

In reality, the investigation of the loss coefficient and torque from experiments will take long time and a lot of money. In this research, the numerical study of loss coefficient and torque of a butterfly valve was carried out by using commercial fluid dynamics software FLUENT. The study focuses on the investigation of the steady and statistical properties of the flow. The simulation was done for 5 different positions of valve disk which are $0°$, $30°$, $45°$, $60°$ and $75°$. The dynamic analysis was also conducted under 2 conditions of butterfly valve's speed, consisting in normally and rapidly rotated condition. The experiment was done under the butterfly valve's size of 150 millimeters diameter at the position of $45°$, $60°$ and $75°$ of the valve. These values will verify the results from the numerical method. The characteristic of the loss coefficient and torque behavior of the flow across the butterfly valve can be analyzed from this study.

Chapter 2 Theory

2.1 Head Loss

Head loss is a measure of the reduction in the total head of the fluid as it moves through a fluid system. It can be explained as the energy equation for steady incompressible flow

$$\frac{P_1}{\gamma} + \alpha_1 \frac{V_1^2}{2g} + Z_1 = \frac{P_2}{\gamma} + \alpha_2 \frac{V_2^2}{2g} + Z_2 + h_L \qquad (2.1)$$

Where $\frac{P}{\gamma}$ is a pressure head

γ is a specific weight

$\frac{V^2}{2g}$ is a velocity head

Z is an elevation head

h_L is a head loss

Head loss is unavoidable in real fluids. It is presented because of the friction between the fluid and the walls of the pipe and the friction between adjacent fluid particles as they move relatively one to another. Frictional loss is that part of the total head loss that occurs as the fluid flows through straight pipes. However, most pipe system consists of more than straight pipes. The other components such as bends, valves and gates etc. installed into the system add head losses to the overall head loss. The head loss associated with flow through a valve is commonly known as minor loss. In general, the head loss information for all components is given in dimensionless form and based on experimental data as shown in table 2.1

	Type pf Component	K_L
Tee	Line flow, flanged	0.2
	Line flow, threaded	0.9
	Branch flow, flanged	1
	Branch flow, threaded	2
Elbows	Regular 90, flanged	0.3
	Regular 90, threaded	1.5
	Long radius 90, flanged	0.2
	Long radius 90, threaded	0.7
	Long radius 45, flanged	0.2
	Regular 45, threaded	0.4
Valves	Globe, fully open	10
	Angle, fully open	2
	Gate, fully open	0.15
	Gate, ¼ closed	0.26
	Gate, ½ closed	2.1
	Gate, ¾ closed	17

Table 2.1 : The examples of Loss coefficient for pipe components

The most common method is to specify the loss coefficient, K_L which is defined as

$$K_L = \frac{h_L}{\left(V^2/2g\right)} = \frac{\Delta P}{\frac{1}{2}\rho V^2} \tag{2.2}$$

It can be shown as

$$\Delta P = K_L \frac{1}{2}\rho V^2 \tag{2.3}$$

Or

$$h_L = K_L \frac{V^2}{2g} \tag{2.4}$$

2.2 The Previous Researches of the Butterfly Valve

The study of the flow past the butterfly valve has been done for long times. In the early period, only experiments were carried out to investigate the characteristics of the flow through the butterfly valve. Due to limit of technology, the numerical method was not popular yet. In 1988, Eom K. studied research named " Performance of

Butterfly Valves as a Flow Controller ". The study investigates the performance of two different configurations of butterfly valve, consisting of perforated and solid blade as shown in Fig 2.1. The total pressure loss, ΔP across the valve is measured in constant $4''$ pipe diameter as shown in Fig 2.2 to investigate the characteristic of loss coefficient of every 10 degrees from 0 to 90 degrees. From experimental results, it was found that the maximum loss coefficient of a solid disk is a little larger than a perforated disk when the valve approached the closed position. These results support the suitability of a butterfly valve as a good flow controller.

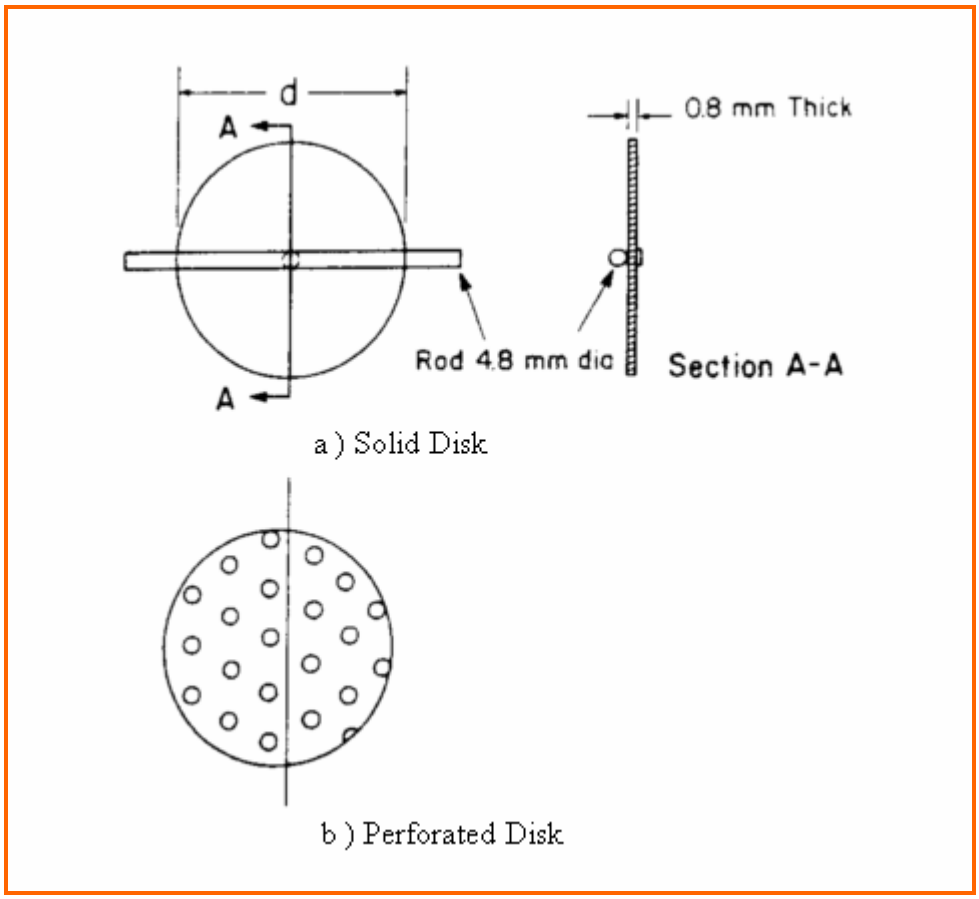

Figure 2.1 : The blade configuration

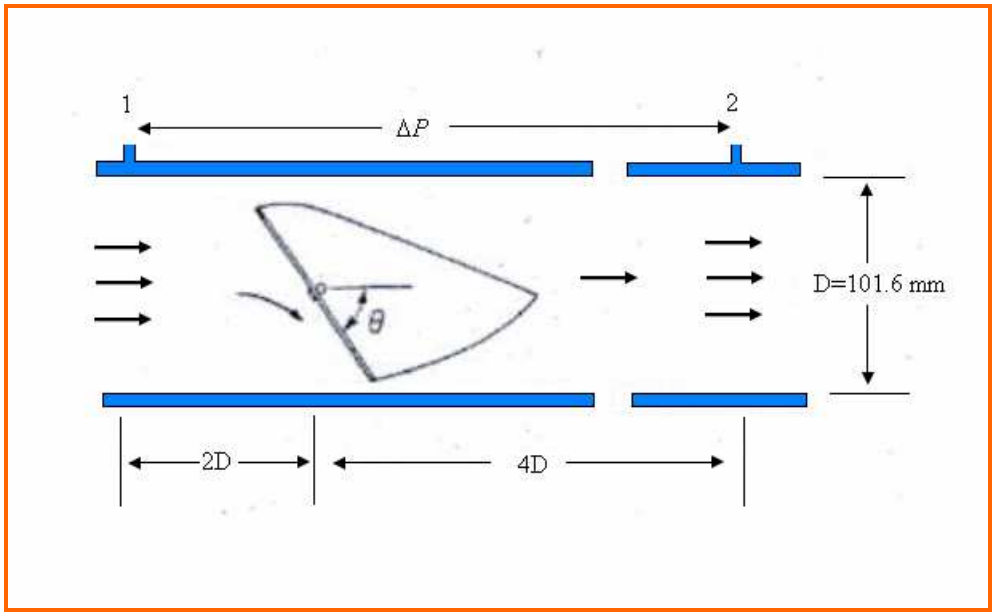

Figure 2.2 : The flow across butterfly valve

The butterfly valve becomes very popular in various kinds of piping system. The valve may be installed in different conditions such as in incompressible and compressible flows. It also can be set up by different types of the valve disk. Due to effect of the flow conditions and the valve configuration, the flow past the butterfly valve may be different. So Morris M. J. and Dutton J. C. have conducted research named " Compressible Flow field Characteristic of Butterfly Valves " in 1989. Two basic valve disk geometries, shown in Fig 2.3 , were used: a generic biconvex circular arc profile and the mid plane cross-section of a prototype butterfly valve. The research focused on the actual flow field within a butterfly valve and the influence of the corresponding flow phenomena on the operating characteristics of the valve. This experiment was carried out with two-dimensional valve model, in a rectangular wind tunnel test section. For these flow conditions, the Reynolds number and Mach number varied over the approximate ranges $13\times10^5 \le \mathrm{Re} \le 5.2\times10^6$ and $0.04 \le M \le 0.64$, respectively. The experimental results showed that the flow field through butterfly valve was extremely complex and depended on the valve disk geometry, the operating pressure conditions and the disk angle. The flow field may consist of regions of strong pressure gradients, shock waves, flow separation and reattachment as show in Fig 2.4.

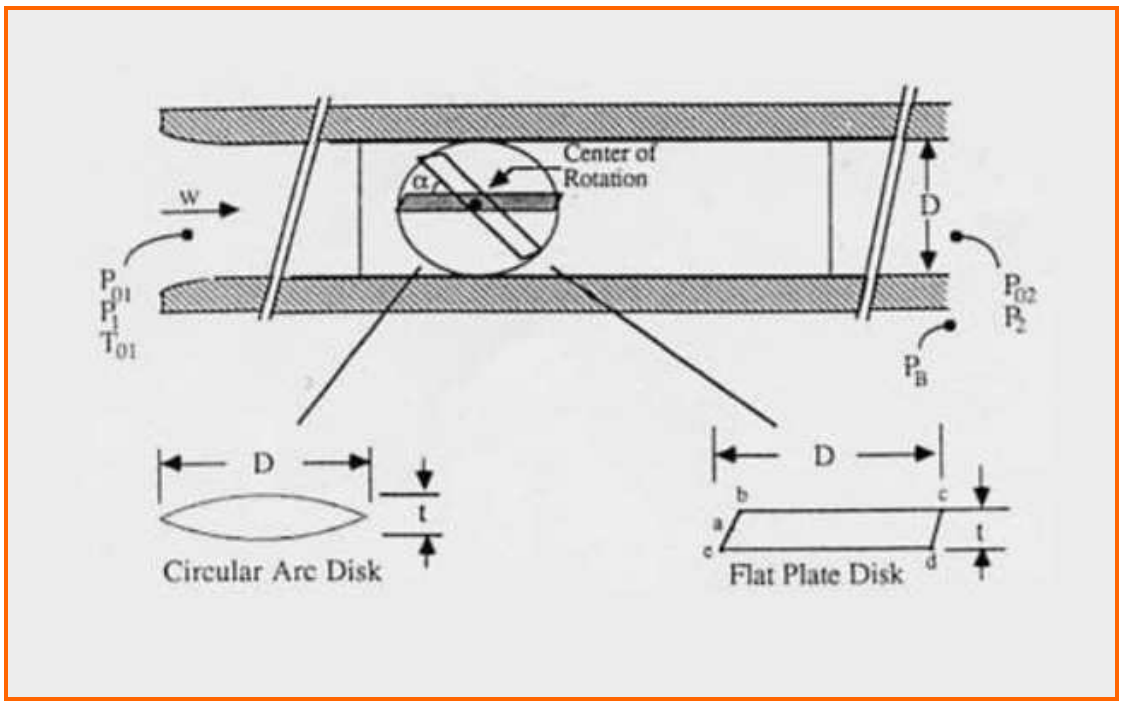

Figure 2.3 : The schematic of the two-dimensional wind tunnel test section used in the butterfly valve flowfield studies

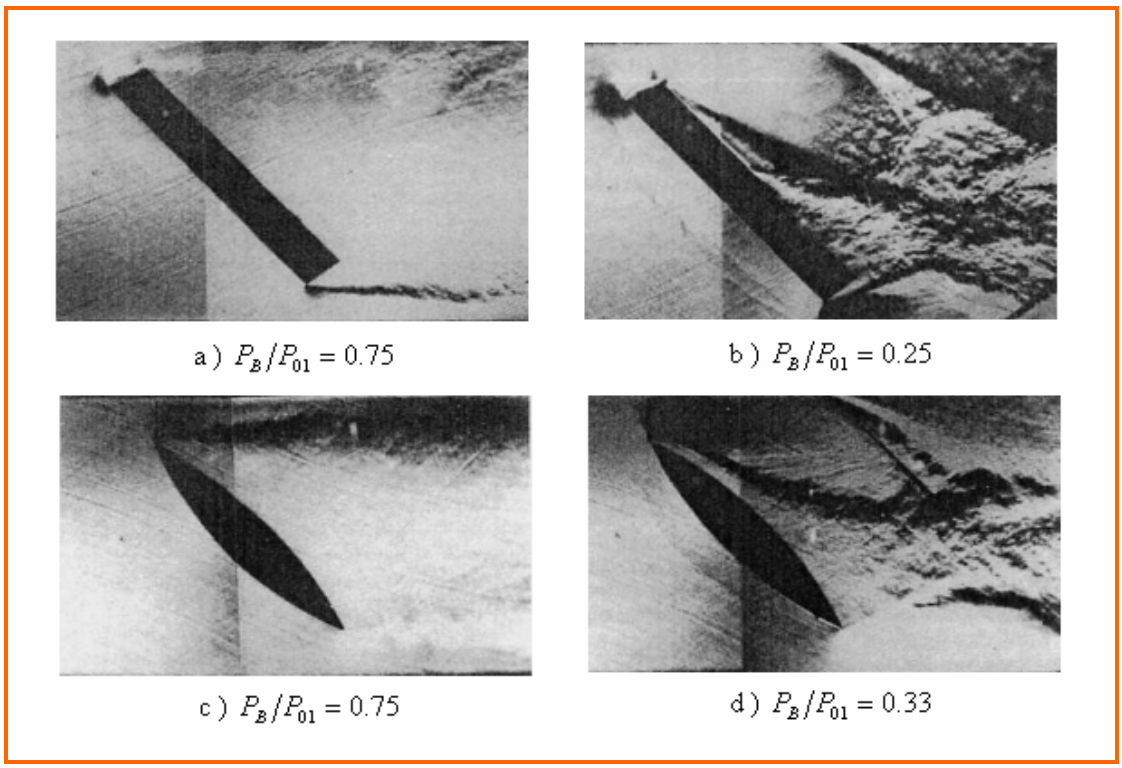

Figure 2.4 : The schlieren photographs of the flow field at $\alpha = 45°$ for the flat plate valve disk : (a) $P_B/P_{01} = 0.75$, (b) $P_B/P_{01} = 0.25$ and for the circular arc valve disk : (c) $P_B/P_{01} = 0.75$, (d) $P_B/P_{01} = 0.33$

Torque is another standard parameter of the butterfly valve. To investigate the torque characteristics, In 1989, Morris M. J. and Dutton J. C. studied " Aerodynamic Torque characteristics of Butterfly Valves in Compressible Flow ". This study focused on an experimental investigation of the aerodynamic torque characteristics of three-dimensional and two-dimensional valve at choked and unchoked operating points. The experiment, as shown in Fig 2.5, run by two types of disk consisting of flat plate type and circular arc profile type, showed in Fig 2.6. The valve disk angle was varied in a range from fully opened, $\alpha = 0°$ to nearly closed position, $\alpha = 70°$, under condition of Mach number $0.04 \le M \le 0.69$ and Reynolds number $1.3\times10^5 \le \mathrm{Re} \le 5.2\times10^6$. The experimental results showed that a three-dimensional valve flow field is different from a two-dimensional model flow field. The differences occur such as the separated and reattachment points etc. The torque characteristic of butterfly valve is strongly related to the separation and reattachment characteristics of the flow. However, at both valve disk angles corresponding to a fully opened and fully closed positions, the influence of disk shape for valves is minimum due to the balance of aerodynamic forces.

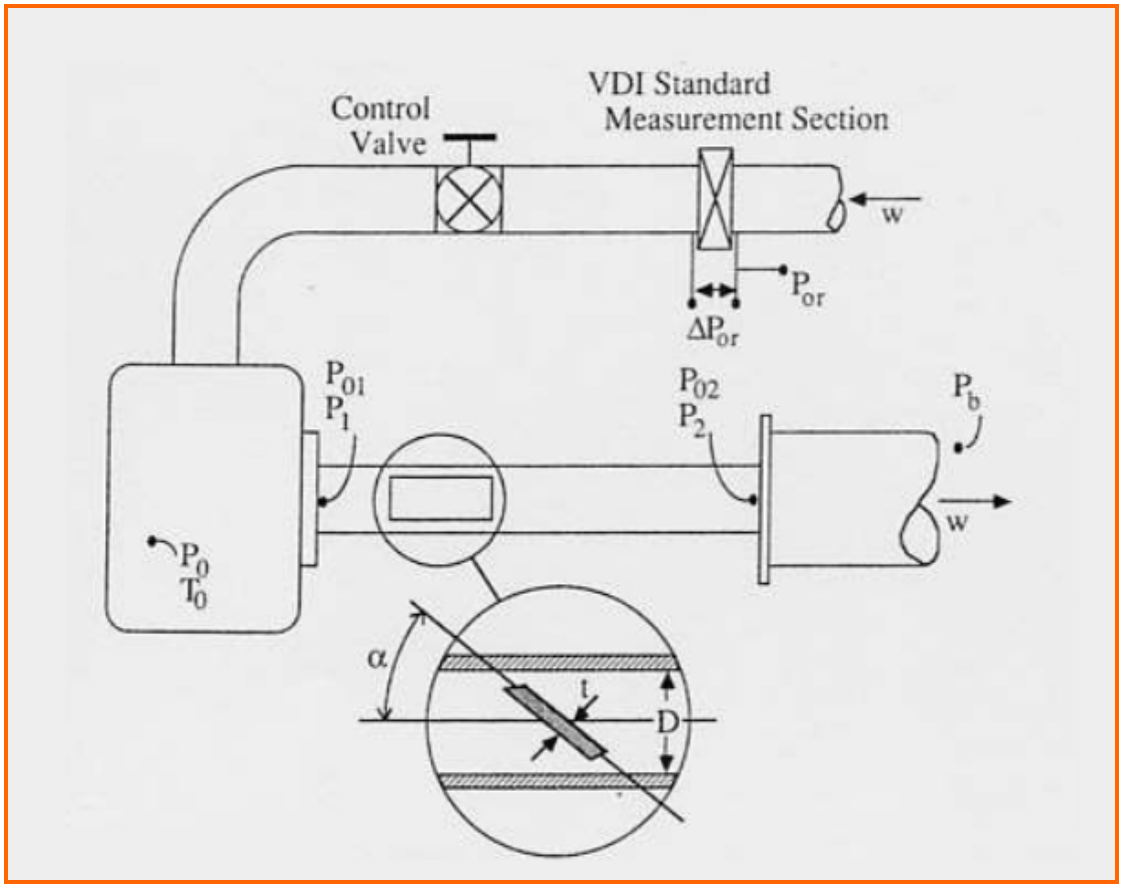

Figure 2.5 : The schematic of experimental apparatus and nomenclature for model valve experiments

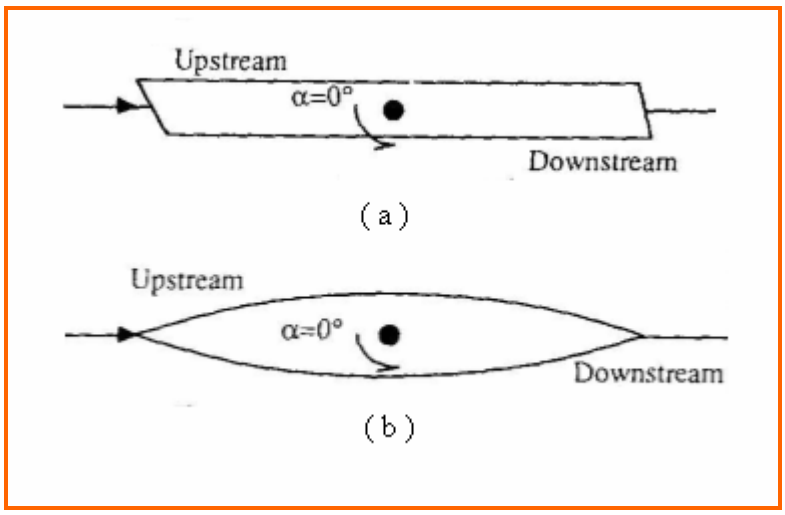

Figure 2.6 : The blade configurations

In reality, the butterfly valve will be involved with many types of device in the piping system. Elbow is one of them. In 1991, Morris M. J. and Dutton J. C. have done research named "An Experimental Investigation of Butterfly Valve Performance Downstream of an Elbow ". This investigation focused on the operating characteristics of three butterfly valve models. The pipe Reynolds numbers were approximately 3×10^4 to 7×10^5. The angles of valve disk were positioned in range from 0 deg(fully opened) to 70 deg(nearly closed). The operating characteristics of interest comprised the dimensionless static pressure drop, mass flow-rate capacity and aerodynamic torque, reported as a dimensionless torque, $C_T \equiv \frac{T}{D^3(P_1 - P_2)}$, where T is the aerodynamic torque and D is the valve diameter. The valves and the elbow were spaced at the distances of 2, 4 and 8 pipe diameter. This investigation used air as the working fluid through the system which was setup as shown in Fig 2.7. The results show that the operating characteristics of a butterfly valve can be changed dramatically by valve/elbow interaction. When the valve is located 2 pipe diameters downstream of the elbow, the operating characteristics are immediately affected by the relation valve/elbow orientation. However, at a spacing of 8 pipe diameters the effect of the elbow on the valve operating characteristic is small. An example of experimental results is shown in Fig 2.8.

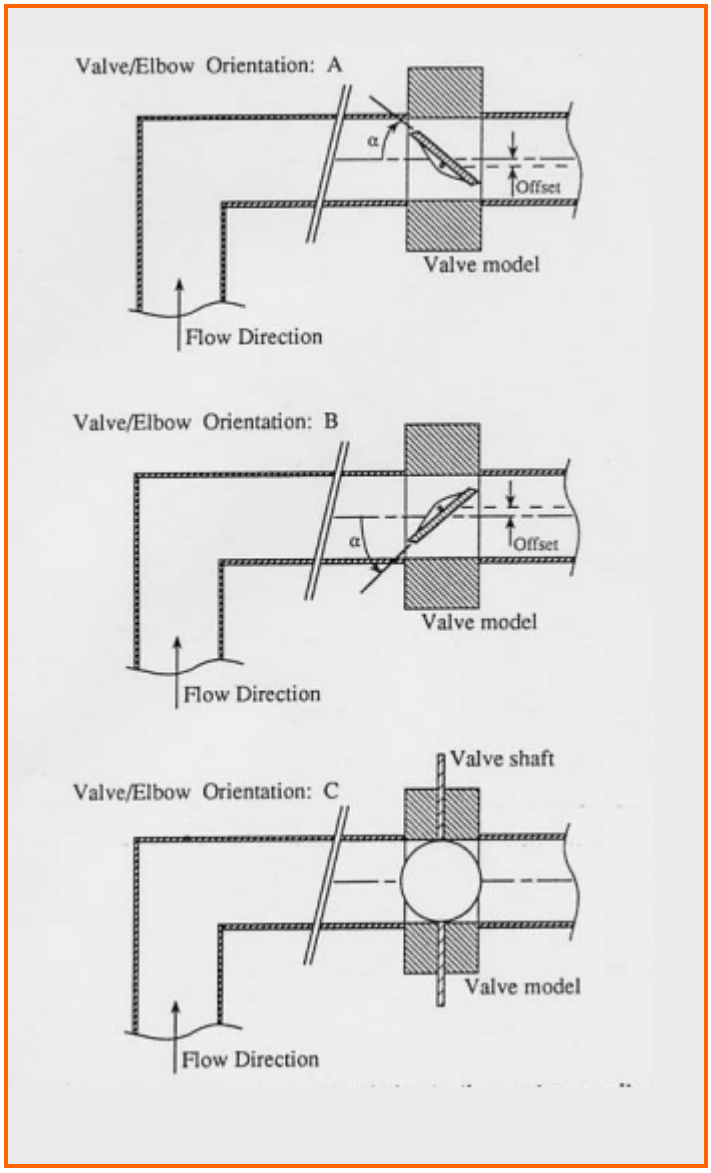

Figure 2.7 : The three valve orientations relative to the upstream mitered elbow

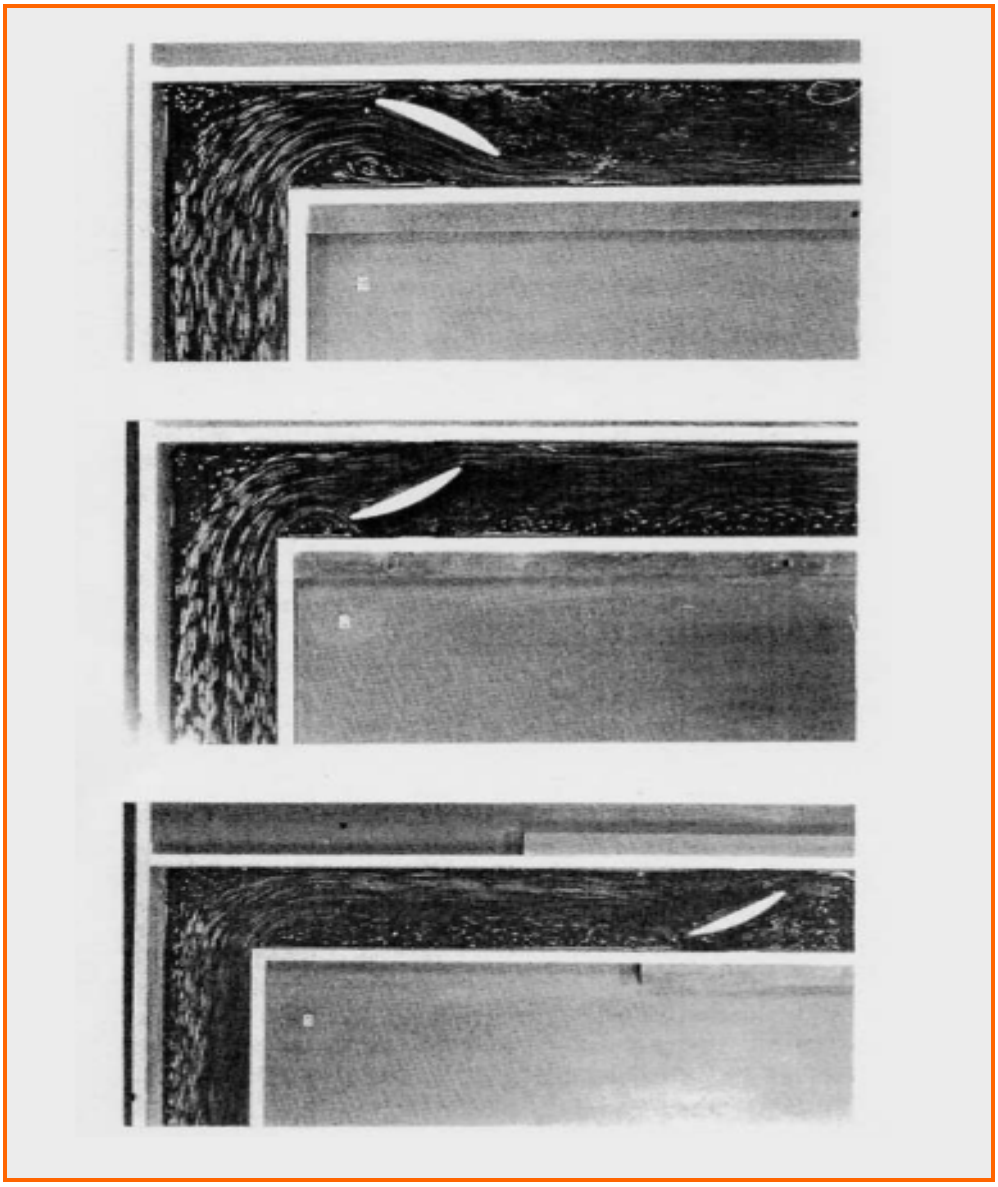

Figure 2.8 : The typical results from a water flow across the butterfly valve

After the numerical method becomes famous, many practical engineering works as well as the flow past the butterfly valve were solved to investigate the characteristic of the flow-field. In 1996, Huang C. and Kim R. H. did a research named “Three-dimensional Analysis of Partially Open Butterfly Valve Flows “. This study focused on fluid flows through a circular disk in a circular pipe as shown in Fig2.9. The main parameters which were used were the pipe diameter D = 25.4 mm, and α defined as valve disk angle from 0 to 90 degree. W_{in} was velocity inlet, which was 0.9144 m/s. The water was used as an operating fluid. The inlet turbulent kinetic energy was $1.351\times10^{-3}\, m^2/s^2$ and kinetic energy dissipation was $9.176\times10^{-3}\, m^2/s^3$. These two parameters were used with a two equations of $k-\varepsilon$ model. From numerical results, it was found that the computational investigation agrees with the results from the experiment. The results such as velocity vector profile shown in Fig 2.10 pointed out that the flow field through the butterfly valve was very complex and depended upon the valve disk angle.

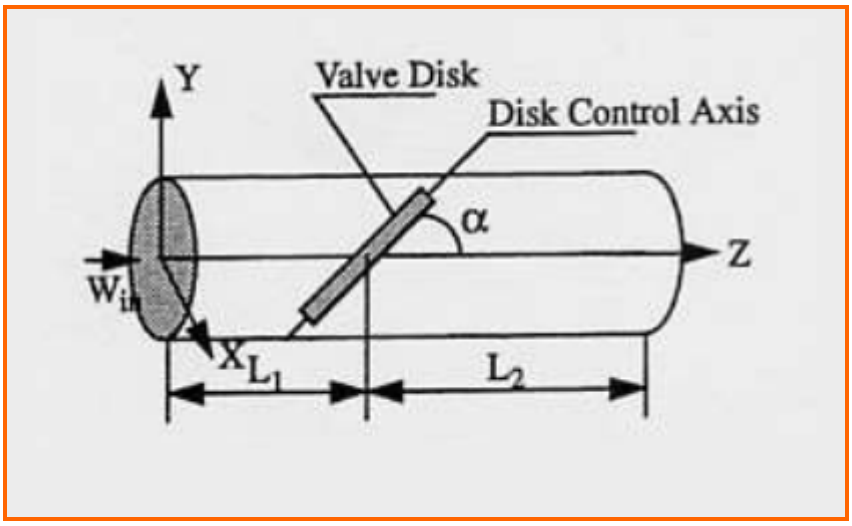

Figure 2.9 : The simplified model and coordinate system

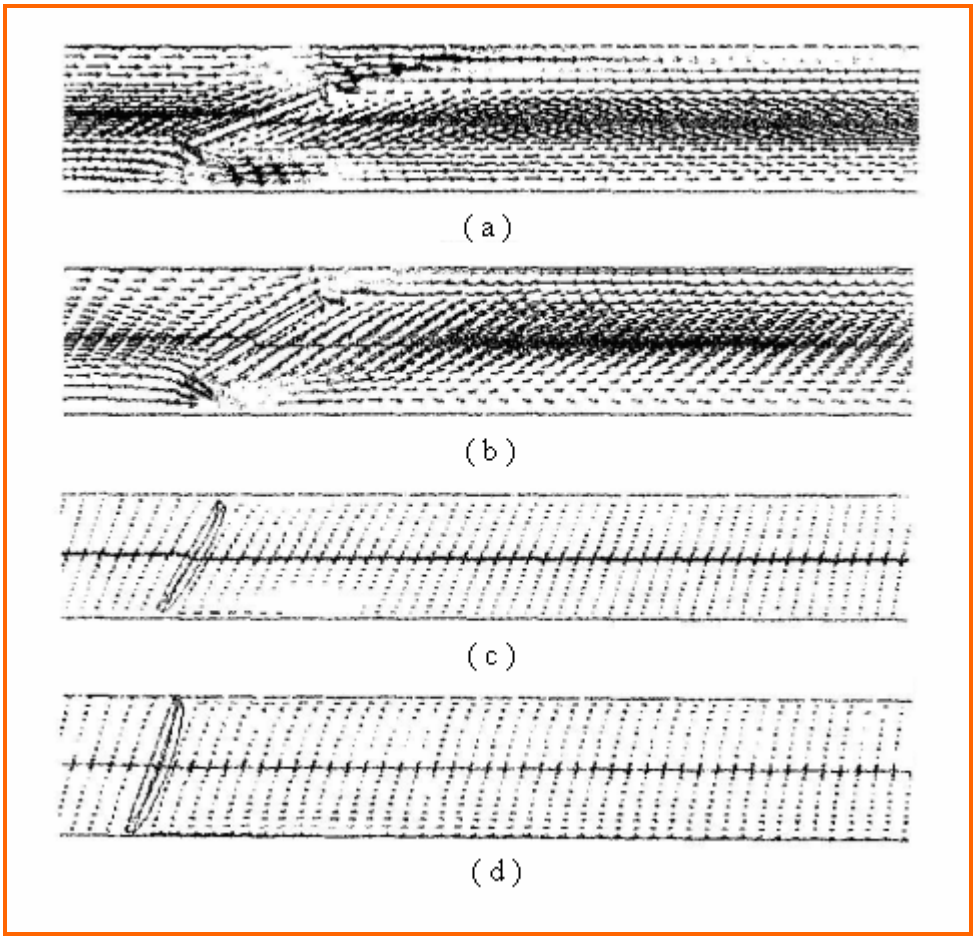

Figure 2.10 : The velocity vector on a Y-Z plane, with the valve disk angle (a) 20° , (b) 30° , (c) 60° and (d) 70°

In 1999, Solliec C. and Danbon F. have carried out research named " Aerodynamic Torque Acting on a butterfly valve. Comparison and choice of a Torque Coefficient ". In reality, when the valve is closed downstream of an elbow, the valve

pressure drop is not well defined. So this study focused on the investigation of the characteristics of torque coefficient, C_T instead of the pressure drop. These tests were conducted in an opened air circuit as shown in Fig 2.11. The valve disk angle, α was set from the fully opened position, $\alpha = 0°$ to the closure $\alpha = 90°$. The inlet duct Reynolds number was set from the range $5\times10^4 \le \mathrm{Re} \le 10^6$ through two different types of elbows as illustrated in Fig 2.12. From the results as shown in Fig 2.13, it was found that the results were very sensitive to the method of torque coefficient. The classical approach, which consists on the method of pressure drop, is only suitable in a straight pipe. When a hydraulic singularity is added closed to the valve, the use of torque coefficient is preferable.

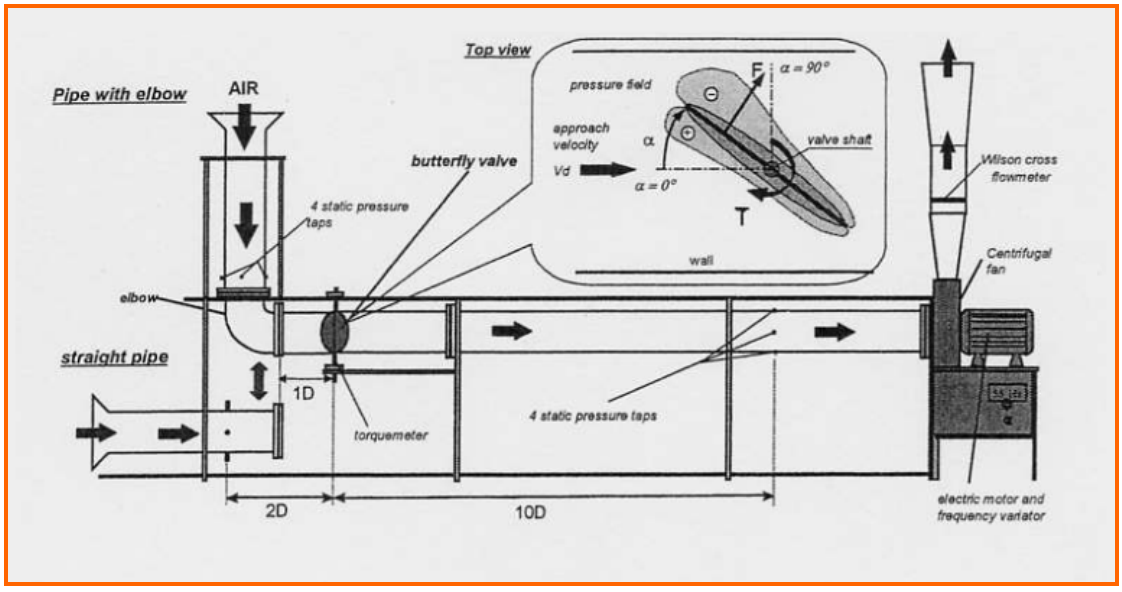

Figure 2.11 : The schematic view of the test bench and nomenclature

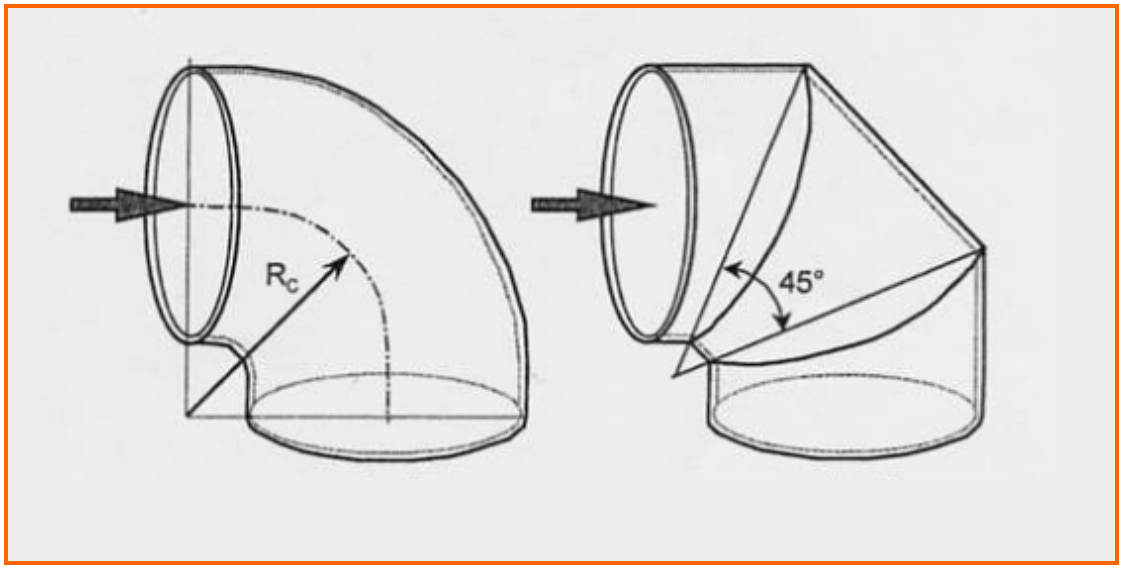

Figure 2.12 : The cross section of the two $90°$ elbows

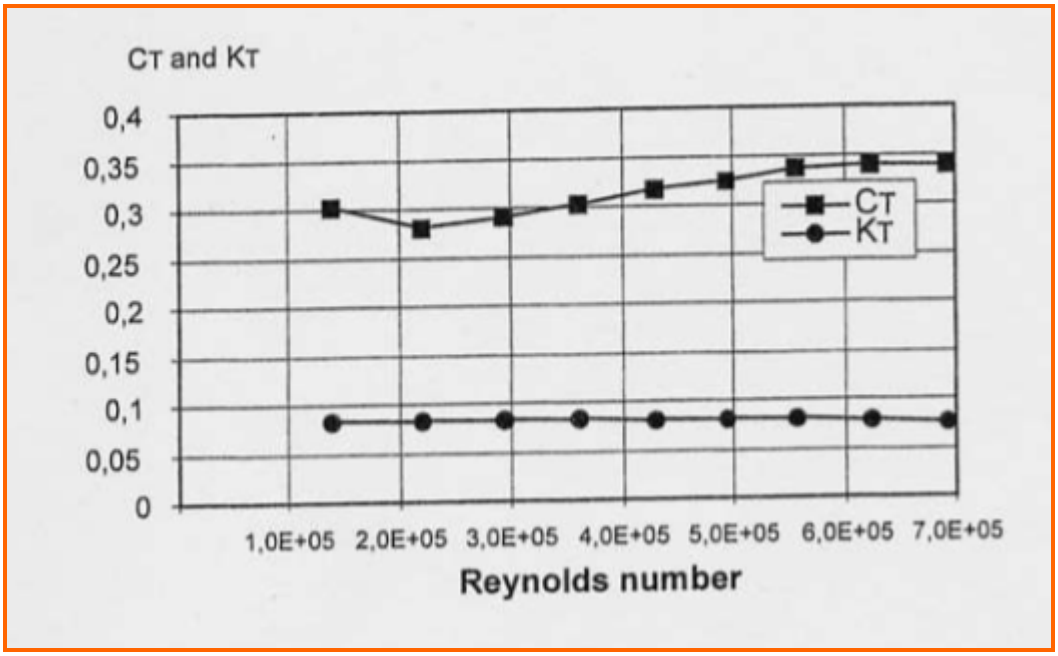

Figure 2.13 : The relation between the mean torque coefficient and The loss coefficient

The study of the flow through the butterfly valve, near the elbow was furthered in 2000. Solliec C. and Danbon F. have done research named " Aerodynamic Torque of a butterfly Valve- Influence of an Elbow on the Time-Mean and Instantaneous Aerodynamic Torque ". The object of this research was to analyze the fluctuations of the instantaneous torque according to the valve/elbow spacing, of the aperture of the valve and to make recommendations for the installation of this kind of flow control unit. A method of direct measurement by torque-meter and an indirect method by integration of the pressure force on the faces of the valve gave access to the time-mean and instantaneous torque on the valve shaft. The experiment as shown in Fig 2.14 was carried out with valve disk angle from $0° - 90°$. With air as working fluid, the test was conducted by the inlet duct Reynolds number $5 \times 10^4 \le \mathrm{Re} \le 10^6$. The pressure distribution on surface of disk was measured by 27 pressure taps as shown in Fig 2.15. From the experimental results, it was found that the mean torque coefficient C_{TP}, calculated by pressure integration and measured by torque-meter showed a good agreement as shown in Fig 2.16. At completely opened position, the elbow induces harmful fluctuations. However these effects would disappear beyond a distance from 8 to 10 times of the diameter of the pipe.

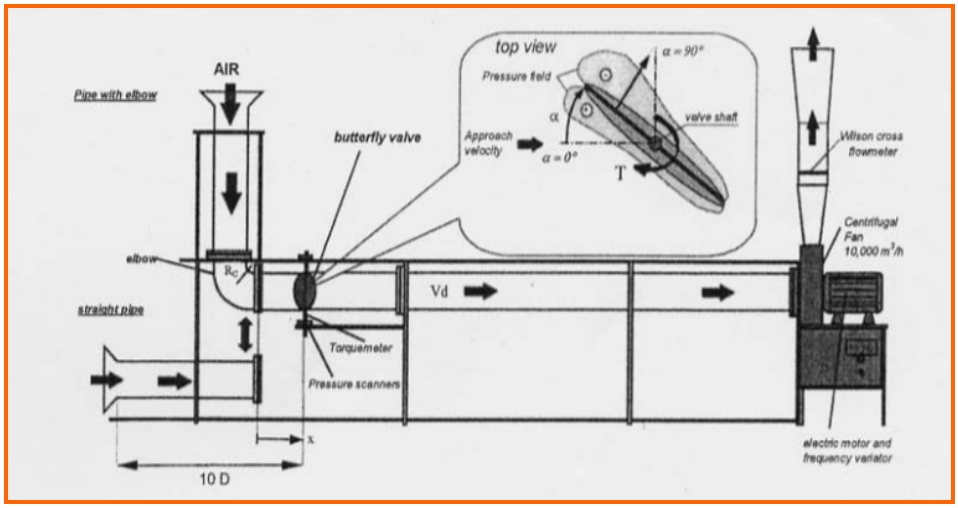

Figure 2.14 : The schematic view of the test bench and nomenclature

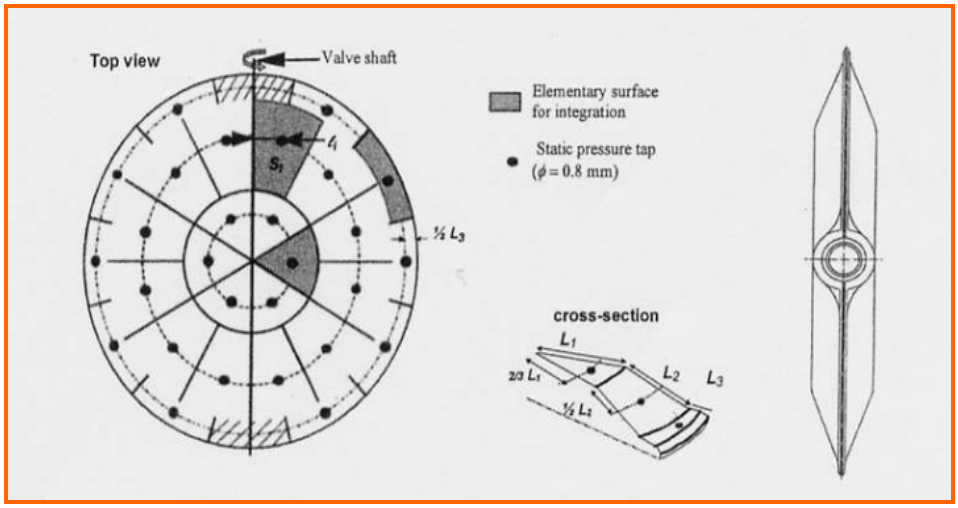

Figure 2.15 : The pressure taps location and cross section of the valve

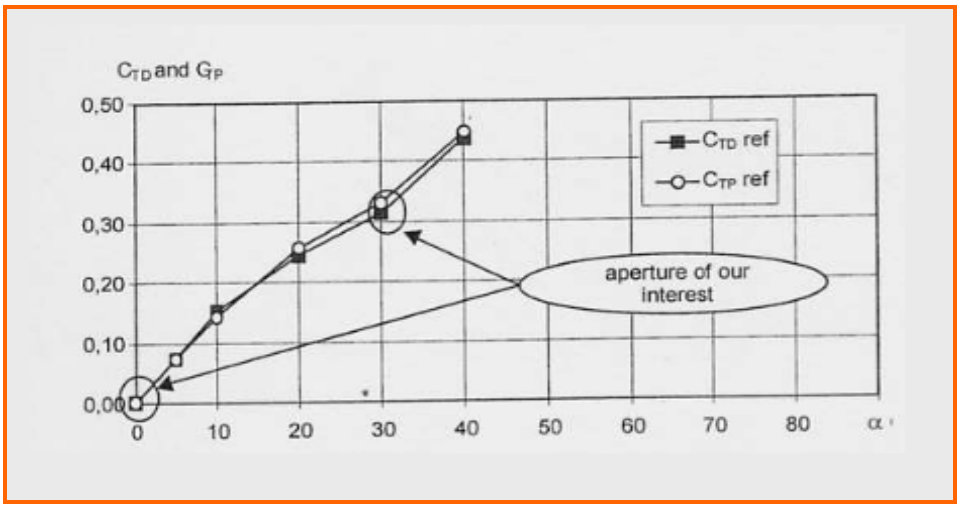

Figure 2.16 : The comparison between time-mean torque coefficients C_{TP} and C_{TD} for different opening angles in the straight pipe configuration

Due to the advance of the numerical method, many turbulent models were created to reach a specific problem. The comparison between different turbulent models was made by Leutwyler Z. and Dalton C. in 2006. They carried out research named " A compressible Flow on a Butterfly Valve Disk in Mid-stoke Position ". The research focused on the prediction of the aerodynamic torque and lift and drag forces on a 2-dimensional model of butterfly valve using computational fluid dynamics package, FLUENT. The investigation was conducted over the disk position 30, 45 and 60 degrees(where 0 degree is the fully closed position) as shown in Fig 2.17. The comparison of disk pressure profile and disk position was made by several turbulent model consisting of $k-\varepsilon$, Spalart-Allmaras, and $k-\omega$ model as shown in Fig 2.18. From the computational results as shown in Fig 2.19, it was found that the flowfield is highly dependent on the different pressure between upstream and downstream of the valve. The vortex characteristic behaves differently in terms of the expansion of the fluid and the angle of the disk. The pressure profiles on the disk were compared to test data in parameters of the lift, drag forces and aerodynamic torque. They compared all reasonably.

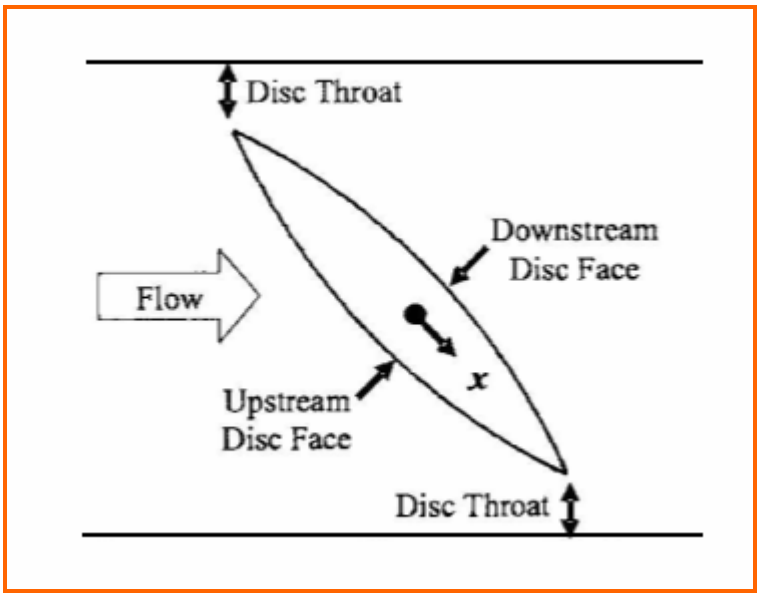

Figure 2.17 : The setup model of numerical simulation

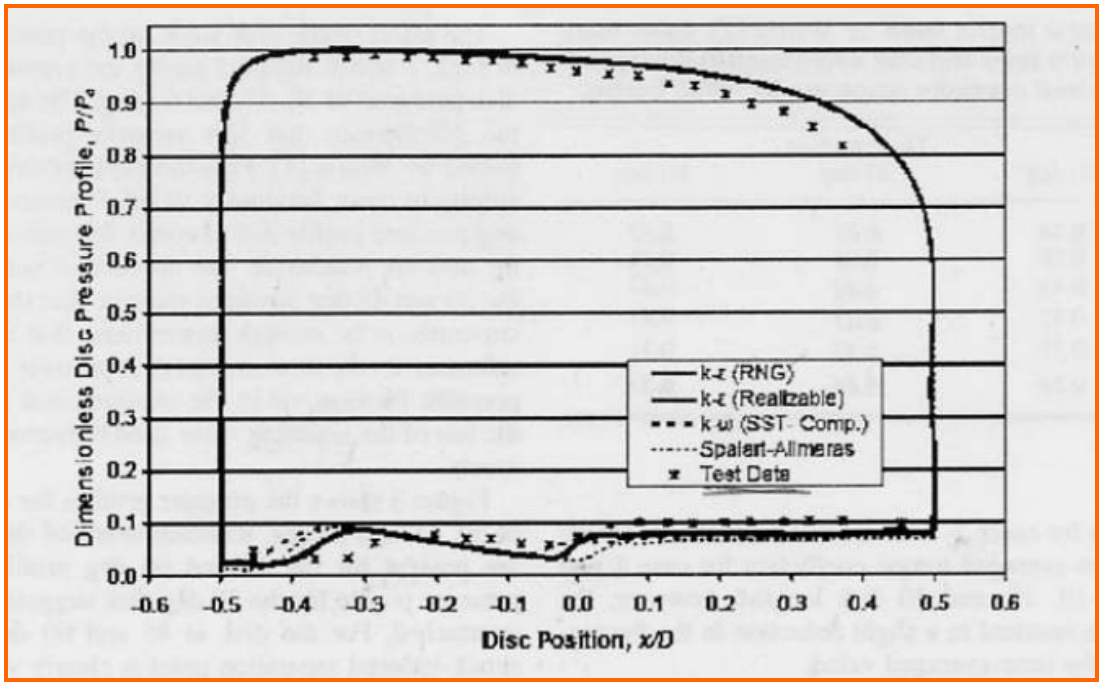

Figure 2.18 : Comparison of the dimensionless pressure profiles of the numerical results for the $k-\varepsilon$, Spalart-Allmaras, and $k-\omega$ model. The test data corresponds to a disk at $45°$ and a pressure ratio of 0.24

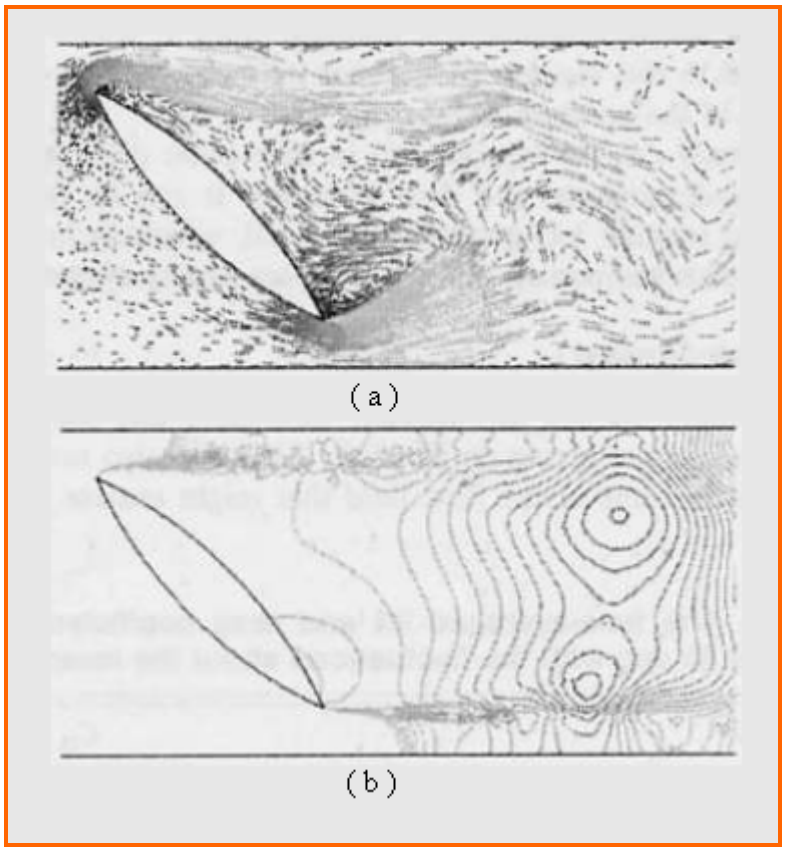

Figure 2.19 : The numerical results of the flow plotted as (a) the mach number vector plot shows the vortex formations caused by the expanding supersonic flow (b) the pressure distribution around the butterfly valve.

Chapter 3 Research procedure and methods

3.1 CFD model setup

Nowadays, numerical method becomes powerful technique and commonly utilized to solve a wide variety of flow problems. The differential equations that govern a flow of Newtonian fluids based on the Navier-Stokes equation. It can be compactly expressed in vector notation as

$$\rho\left(\frac{\partial V}{\partial t}+V\cdot\nabla V\right)=-\nabla p+\rho g+\mu\nabla^2 V \tag{3.1}$$

Along with the continuity equation

$$\nabla\cdot V=0 \tag{3.2}$$

In turbulent flow condition, the fluctuations of the flow particles arise at a small scale and a high frequency. They are too computationally expensive to be modeled directly in practical engineering calculations. The instantaneous governing equations can be time-averaged, ensemble-averaged, or otherwise manipulated to remove the small scales, resulting in a modified set of equations that are computationally less expensive to solve. So the commercial fluid dynamics software FLUENT provides several turbulent model to solve specifically practical problems, shown below

The $k-\varepsilon$ turbulence model has become useful in many practical engineering flow calculations. Economy, robust and reasonable accuracy of this turbulence model explain its popularity in industrial flow and heat transfer simulations. It is a semi-empirical model and the derivation of the model equations relies on phenomenological considerations and empiricism.

The standard $k-\varepsilon$ Model is a semi-empirical model based on model transport equations for the turbulence kinetic energy(k) and its dissipation rate(ε). The model transport equation for k is derived from the exact equation, while the model transport equation for ε was obtained using physical reasoning and bears little resemblance to its mathematically exact counterpart. In the derivation of the $k-\varepsilon$ Model, it was assumed that the flow is fully turbulent, and the effects of molecular viscosity are negligible. The standard $k-\varepsilon$ Model is therefore valid only for fully turbulent flows.

Transport Equations for the Standard $k-\varepsilon$ Model

The turbulence kinetic energy, k and its rate of dissipation, ε are obtained from the following transport equations:

$$\frac{\partial}{\partial}(\rho k)+\frac{\partial}{\partial x_i}(\rho k u_i)=\frac{\partial}{\partial x_j}\left[(\mu+\frac{\mu_t}{\sigma_k})\frac{\partial k}{\partial x_j}\right]+G_k+G_b-\rho\varepsilon-Y_M+S_k \tag{3.3}$$

and

$$\frac{\partial}{\partial t}(\rho\varepsilon)+\frac{\partial}{\partial x_i}(\rho\varepsilon u_i)=\frac{\partial}{\partial x_j}\left[(\mu+\frac{\mu_t}{\sigma_\varepsilon})\frac{\partial\varepsilon}{\partial x_j}\right]+C_{1\varepsilon}\frac{\varepsilon}{k}(G_k+C_{3\varepsilon}G_b)-C_{2\varepsilon}\rho\frac{\varepsilon^2}{k}+S_\varepsilon \quad (3.4)$$

In these equations, G_k represents the generation of turbulence kinetic energy due to the mean velocity gradients. G_b is the generation of turbulence kinetic energy due to buoyancy. The quantity Y_M represents the contribution of the fluctuating dilatation incompressible turbulence to the overall dissipation rate. $C_{1\varepsilon}, C_{2\varepsilon}$ and $C_{3\varepsilon}$ are constants. σ_k and σ_ε are the turbulent Prandtl number for k and ε, respectively. S_k and S_ε are user-defined source terms.

Modeling the Turbulent Viscosity

The turbulent viscosity, μ_t is computed by combining k and ε as follows :

$$\mu_t=\rho C_\mu\frac{k^2}{\varepsilon} \quad (3.5)$$

where C_μ is a constant.

Model Constants

The model constants $C_{1\varepsilon}, C_{2\varepsilon}, C_\mu, \sigma_k$ and σ_ε have the following default values

$$C_{1\varepsilon}=1.44, C_{2\varepsilon}=1.92, C_\mu=0.09, \sigma_k=1.0, \sigma_\varepsilon=1.3$$

These default values have been determined from experiments with air and water for fundamental turbulent shear flows including homogeneous shear flows and decaying isotropic grid turbulence. They have been found to work fairly well for a wide range of wall-bounded and free shear flows. However, the numerical method was used follow the procedure below.

3.1.1 Physical model

A commercial CFD software package, Fluent, was used to simulate the flow passing butterfly valves. These valve, have sizes 150 and 300 mm in diameter that shown in Fig. 3.1 have normally used in any piping system. Not only the model of butterfly valve as shown in Fig 3.2 but also the model of water in the pipe through the valve which is shown in Fig. 3.3 were created using CAD package, Solidworks. In order to get enough entry length and to avoid a non-fully developed flow, an upstream and a downstream length were set to be several times of the pipe diameter. In reality, the economic reason becomes an important factor of research and development. The

symmetric model as shown in Fig. 3.4 was created below under this fact. The size of domain is therefore decreased thus increasing the speed of the numerical simulation.

Figure 3.1 : The valves size 150 and 300 mm

Figure 3.2 : The model of butterfly valve creating by Solidworks

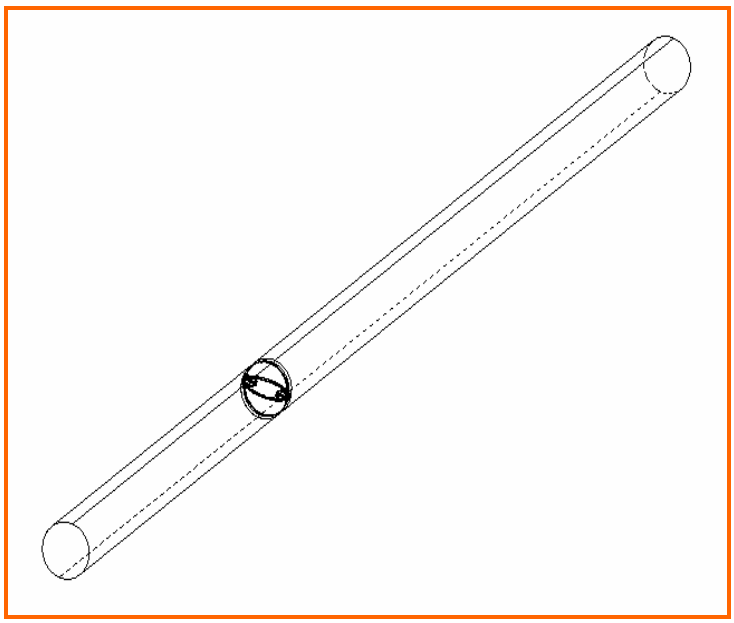

Figure 3.3 : The model of water in the pipe through the valve

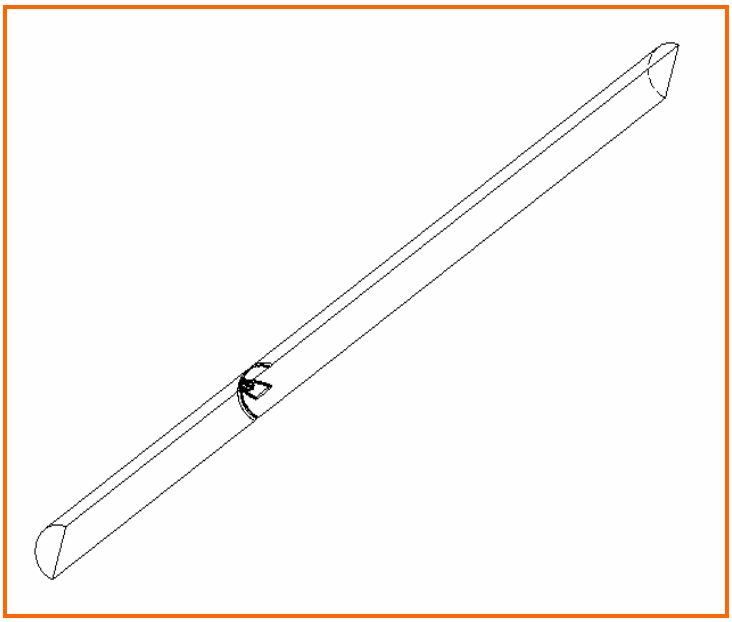

Figure 3.4 : The symmetric model of water in the pipe through the valve

In order to simulate the flow of water over a realistic butterfly valve, an unstructured tetrahedral mesh was created using commercial package, GAMBIT. It consists of the number of the element around 1100000 – 1400000 cells in each case of study. And also the skewness factor of element was set to be not more than 0.97 as shown in Fig. 3.5.

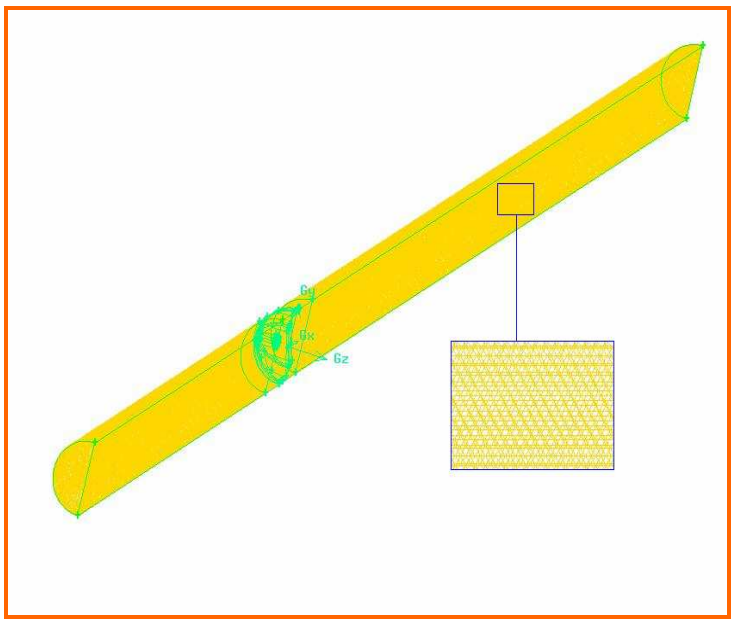

Figure 3.5 : an unstructured tetrahedral mesh on the model of water in the pipe through the valve

The three dimensional analysis would yield a reasonable qualitative result if the effective model were set. The flow was taken to be 3D-symmetry incompressible and turbulent. It was solved by standard k-ε model. The fluid, passing through the valve was water, with density ρ = 999 kg/m^3. The dynamic viscosity was 0.001 kg/ms.

3.1.2 Static Analysis

This study was carried on for 5 positions of valve disk as shown in Fig. 3.6 to investigate the flow-field, loss coefficient and torque characteristic in static condition. The simulation was done under 3 conditions of inlet, consisting of velocity of 1, 2 and 3 m/s in each position. Finally the boundary conditions, using in this study was set to be as in table 3.1 and Fig. 3.7

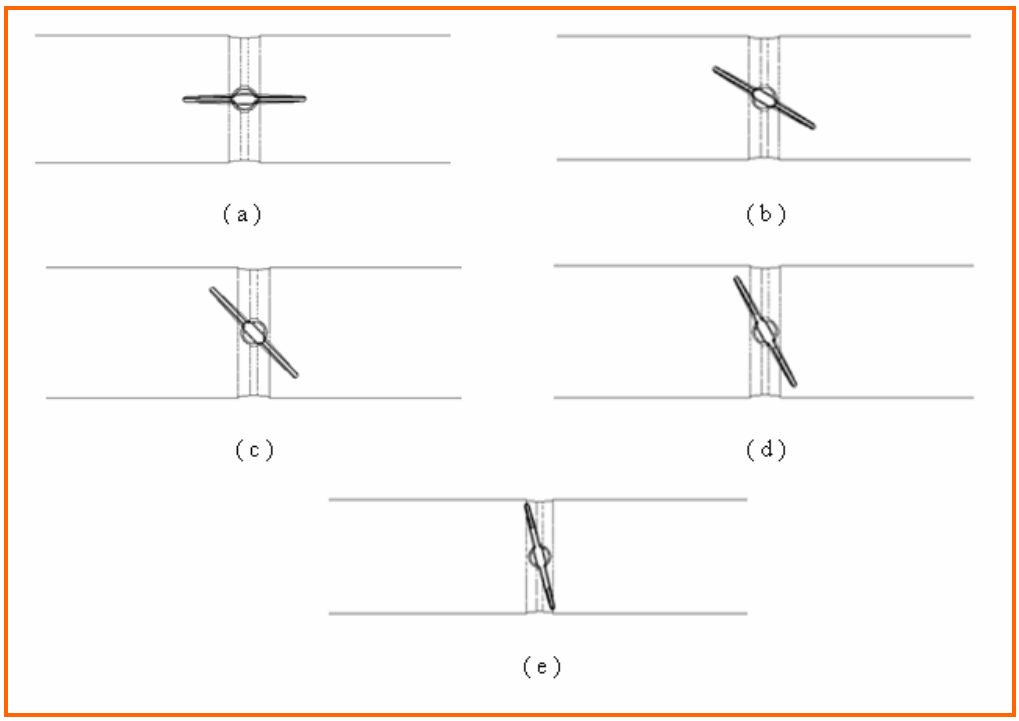

Figure 3.6 : The model of water at (a) 0°, (b) 30°, (c) 45°, (d) 60° and (e) 75° disk position

Surface Domains	Boundary Conditions
Inlet	Velocity Inlet
Outlet	Pressure Outlet
Symmetry	Symmetry
Valve Disk	Wall
Pipe Surface	Wall

Table 3.1 : The boundary condition of each domain of static analysis

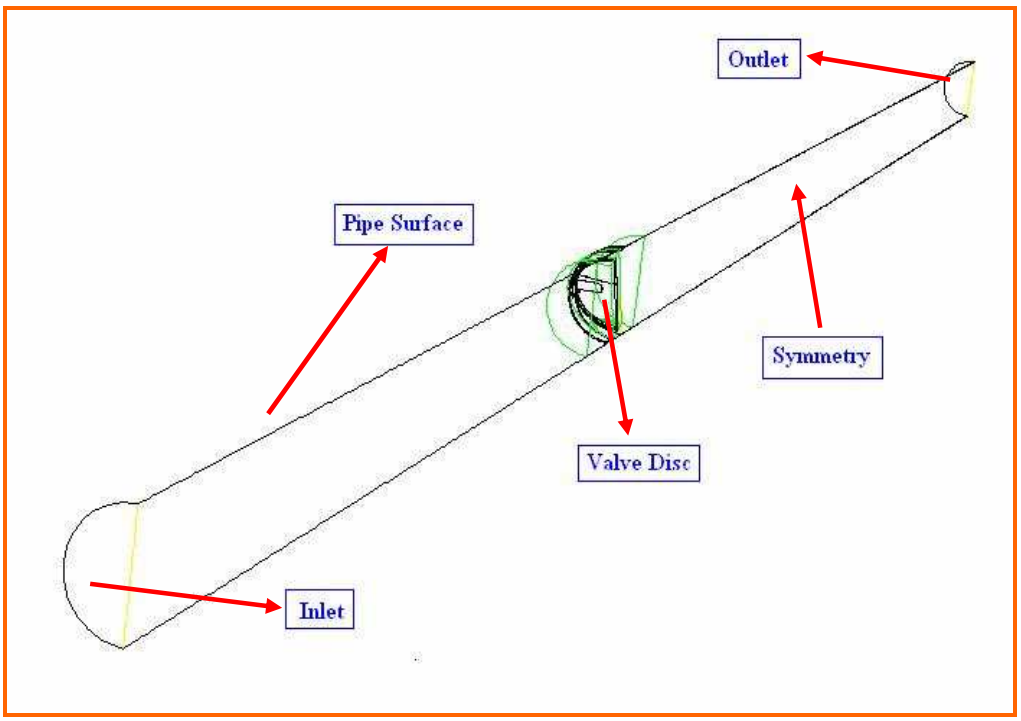

Figure 3.7 : The boundary condition of each domain of static analysis

3.1.3 Dynamic Analysis

A dynamic analysis was done to investigate the flow-field, loss coefficient and torque characteristic in every position of butterfly valve from $0°$ to $180°$. The study conducted under 2 conditions of butterfly valve's speed, consisting of $0.039\,rad/s$ (The butterfly valve would completely close in 40 seconds) and $1.57\,rad/s$ (The butterfly valve would suddenly close in 1 seconds). However, the inlet domain was set under 1 condition, 1 m/s. The boundary conditions, using in this study were set to be as in table 3.2 and Fig. 3.8

Surface Domains	Boundary Conditions
Inlet	Velocity Inlet
Outlet	Pressure Outlet
Symmetry	Symmetry
Valve Disk	Wall
Interior	Interface
Other Surfaces	Wall

Table 3.2 : The boundary condition of each domain of dynamic analysis

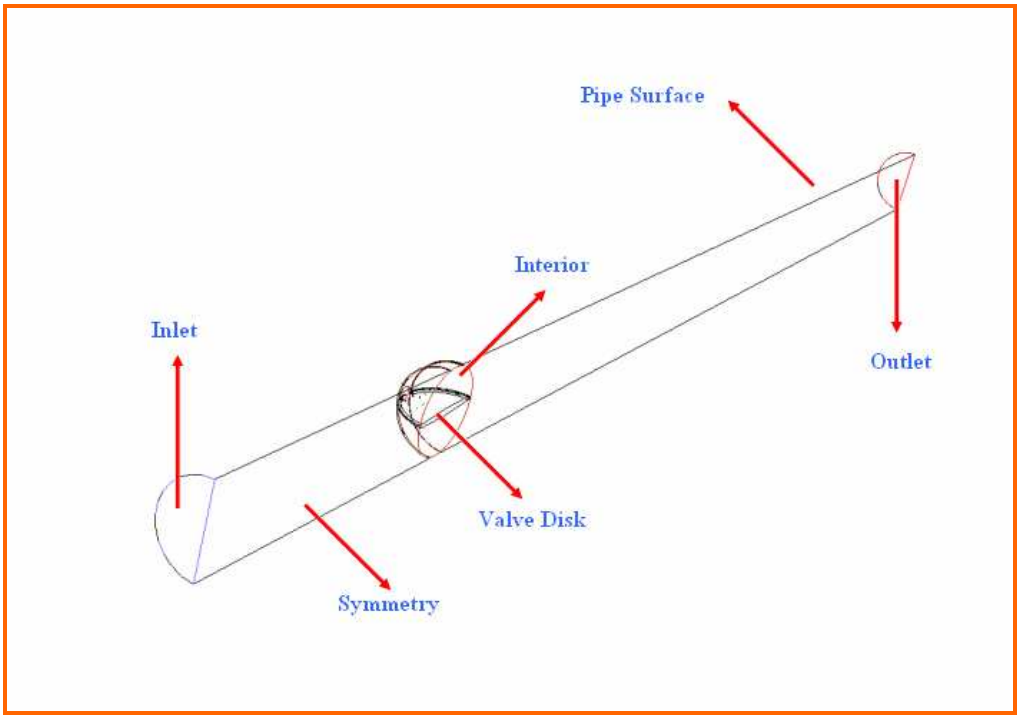

Figure 3.8 : The boundary condition of each domain of dynamic analysis

3.2 The test configuration and experimental method.

The investigation focuses on the operation of three positions of butterfly valve consisting of 45, 60 and 75 degrees. The circular test section is 0.15 m in diameter. The tests were carried out in an open water circuit driven by a 14.7 KW centrifugal water pump. The water pump, showing in Fig. 3.9 has an operating performance curve as shown in Fig. 3.10. A schematic view of the experimental facility is depicted in Fig. 3.11

Figure 3.9 : The 14.7 KW centrifugal water pump

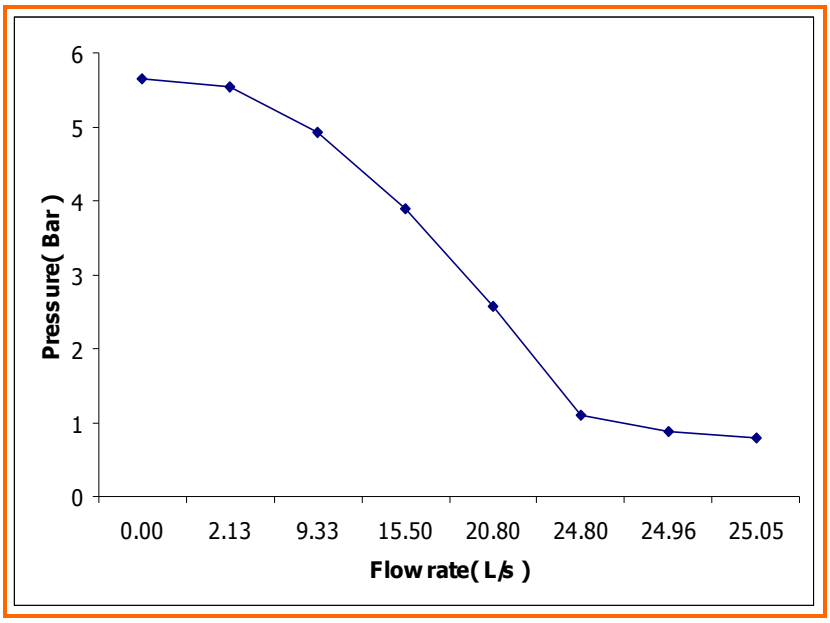

Figure 3.10 : The performance chart of centrifugal water pump

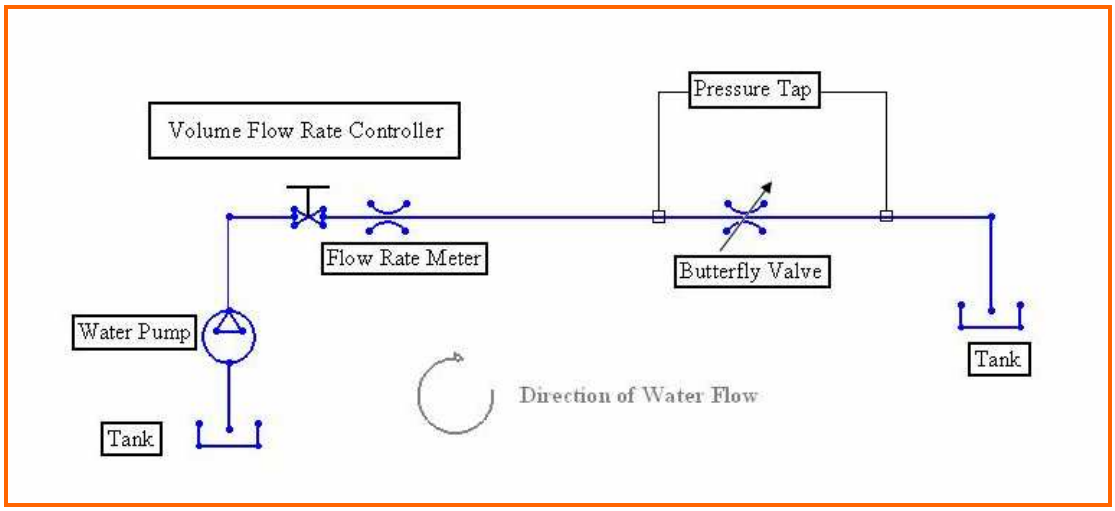

Figure 3.11 : A schematic view of the experimental facility

The volume flow-meter as shown in Fig. 3.12 and also the pressure tap as illustrated in Fig. 3.13 were placed at 14 D downstream and 1 D upstream from butterfly valve. However, the flow rate must be operated in suitable level due to the technical safety in piping system. Three states of flow rate in each position of the disk were illustrated in table 3.3; they were used to measure pressure at inlet and the required torque for changing the disk position. Fig. 3.14 shows torque-meter which has a range from 0-2000 Nm, is located over the butterfly valve.

Figure 3.12 : The flow rate meter at 14 D upstream from butterfly valve

Figure 3.13 : The pressure tab at 1 D upstream from butterfly valve

Position	Volume Flow Rate(L/s)		
(Degree)	State 1	State 2	State 3
45	13.289	19.657	25.753
60	13.418	19.796	25.51
75	10.147	13.504	16.675

Table 3.3 : The values of volume flow rate in each state

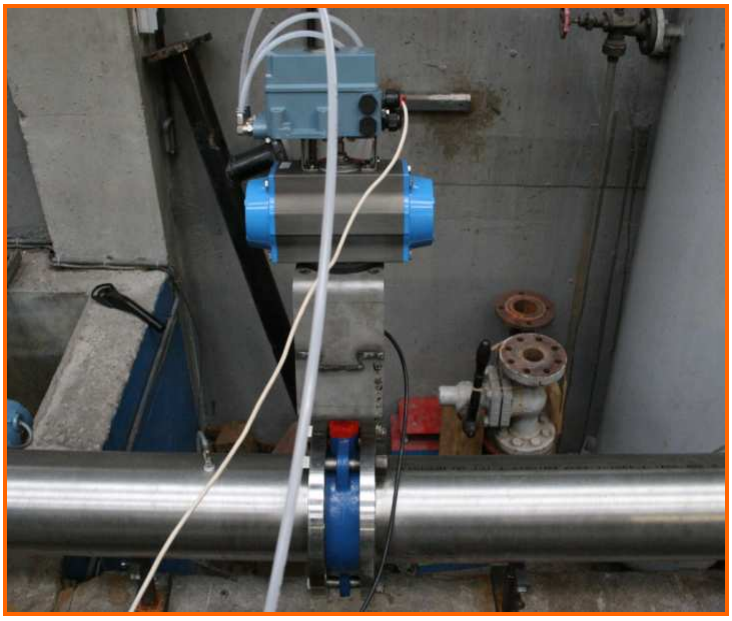

Figure 3.14 : The torque-meter above the butterfly valve

Chapter 4 Results

After the experiments and the simulations were carried out in many conditions of the flow through a butterfly valve, the characteristics of the flow-fields, the characteristics of head loss coefficient and torque are analyzed. The topics in this chapter consist of pressure distributions, velocity distributions, characteristic of head loss coefficient, torque characteristics and the experimental results as shown below.

4.1. The Pressure Distributions

For the butterfly valve of 150 mm in diameter, the simulation for static analysis was done at 5 positions, consisting of $0°$, $30°$, $45°$, $60°$ and $75°$, and for 3 different values of flow-rate: 1, 2 and 3 m/s in each position. From investigation of the flow over this valve, it was found that the pressure is the function of both the value of flow-rate and the position of the butterfly valve. Because the flow is incompressible, the pressure flow-field, shown in Fig 4.1-4.5 will be changed in order the value of velocity at the inlet. In each flow rate condition, the $0°$ position of the butterfly valve causes the lowest stagnation value on its surface therefore it can provide the largest flow rate in this position of the valve. Conversely, the almost closed position($75°$) causes the highest value of stagnation point on the valve surface.

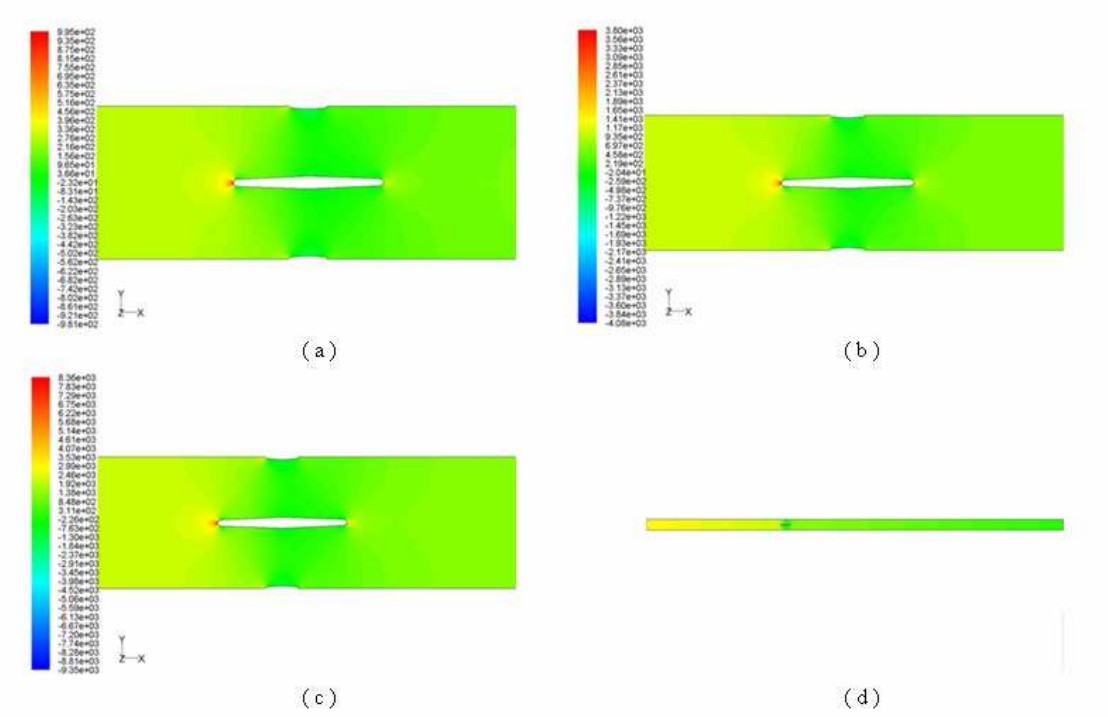

Figure 4.1 : The pressure distribution of the flow at $0°$ position of the 150 mm valve at velocity inlet of (a) $1m/s$, (b) $2m/s$, (c) $3m/s$ and (d) $3m/s$ (large view)

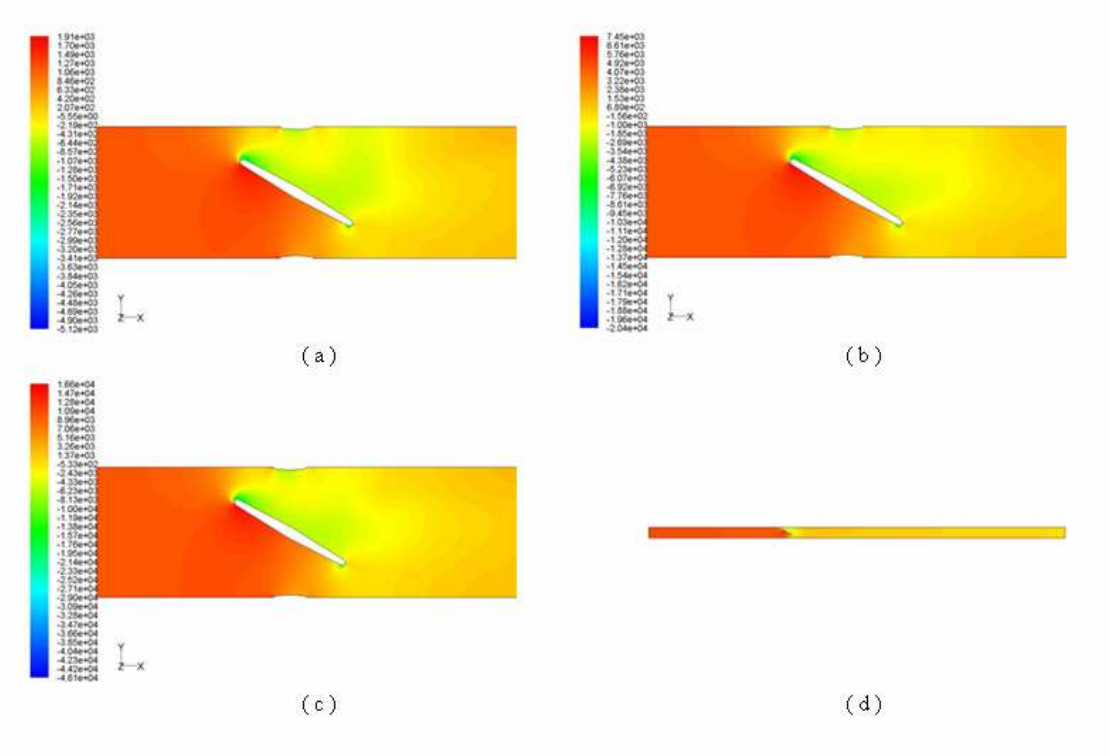

Figure 4.2 : The pressure distribution of the flow at $30°$ position of the 150 mm valve at velocity inlet of (a) $1m/s$, (b) $2m/s$, (c) $3m/s$ and (d) $3m/s$ (large view)

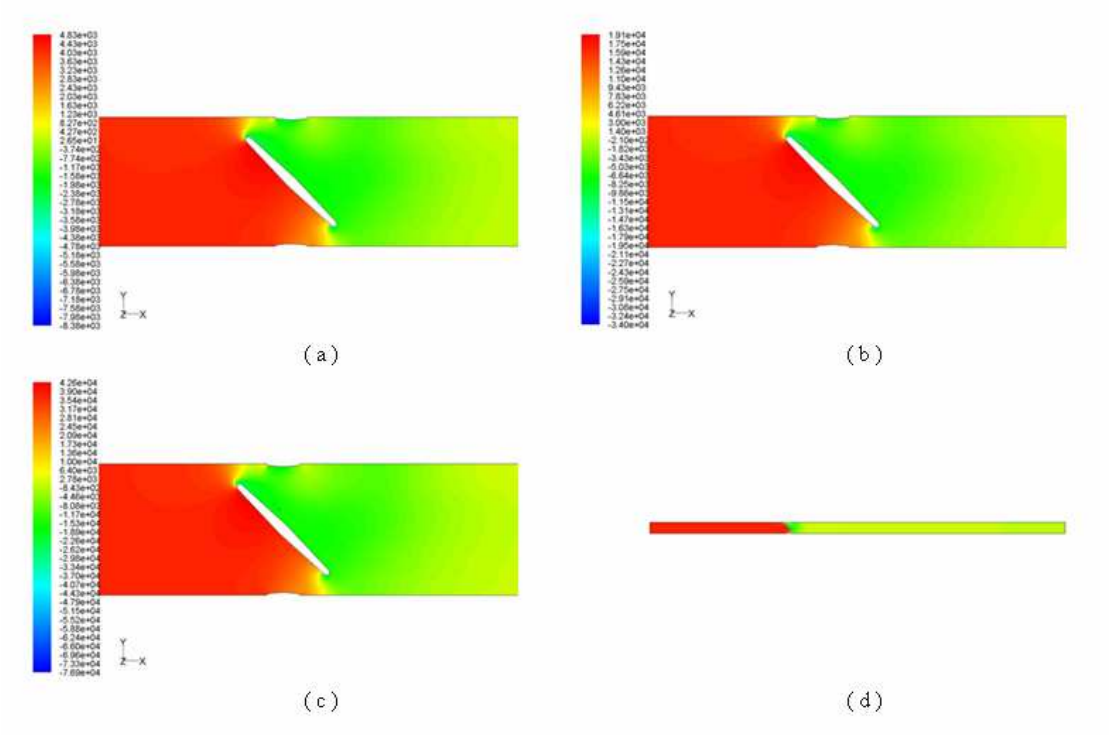

Figure 4.3 : The pressure distribution of the flow at $45°$ position of the 150 mm valve at velocity inlet of (a) $1m/s$, (b) $2m/s$, (c) $3m/s$ and (d) $3m/s$ (large view)

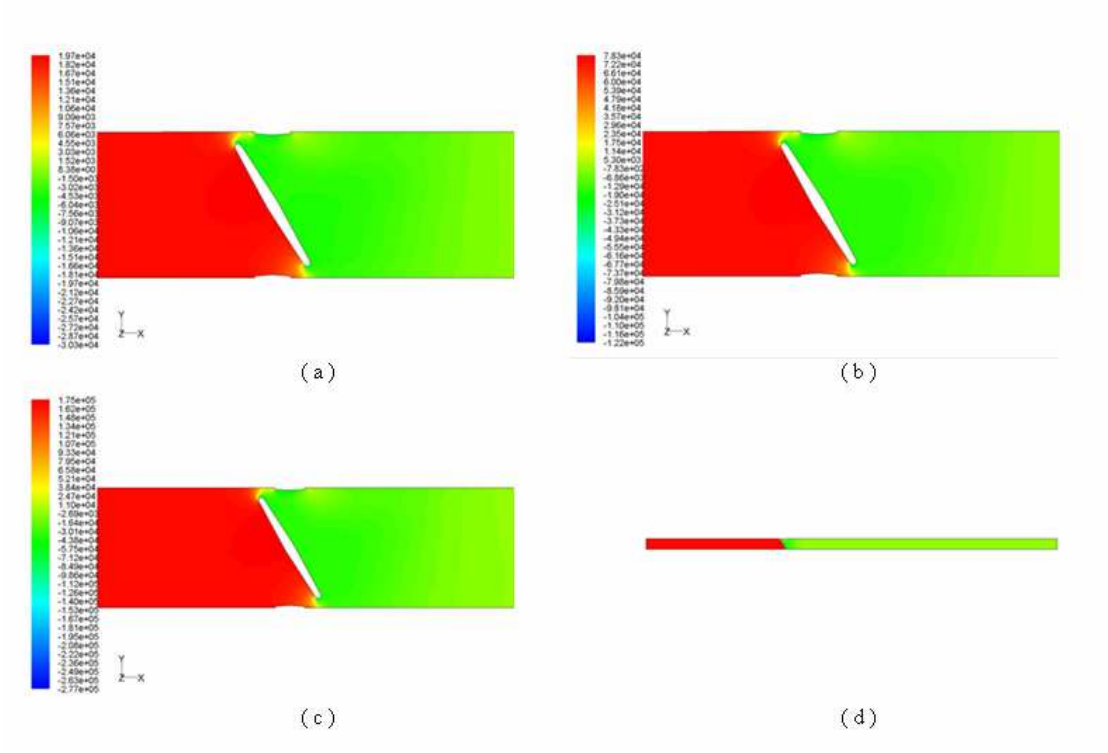

Figure 4.4 : The pressure distribution of the flow at $60°$ position of the 150 mm valve at velocity inlet of (a) $1m/s$, (b) $2m/s$, (c) $3m/s$ and (d) $3m/s$ (large view)

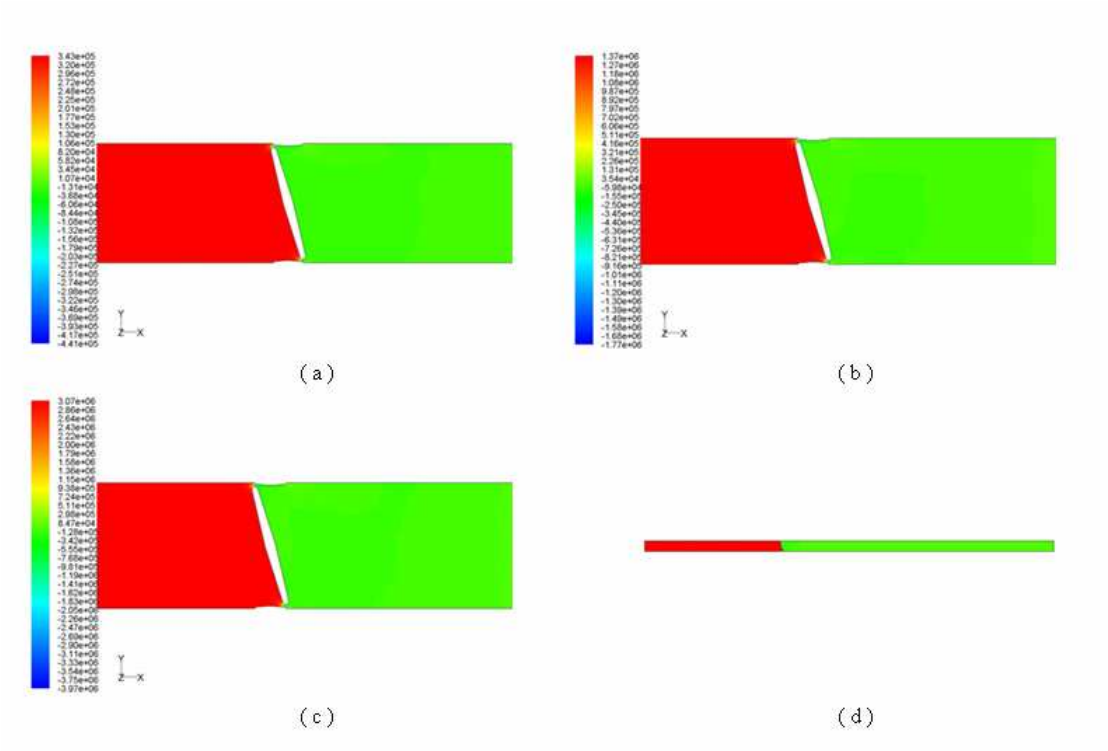

Figure 4.5 : The pressure distribution of the flow at $75°$ position of the 150 mm valve at velocity inlet of (a) $1m/s$, (b) $2m/s$, (c) $3m/s$ and (d) $3m/s$ (large view)

Fig 4.6-4.10 show the pressure distribution of the flow past the 300 mm butterfly valve. Similar to the butterfly valve of 150 mm, the valve of 300 mm in diameter was simulated under 5 positions and 3 loads of flow rate. It was found that the pressure profile of this geometry is very similar to the one obtained for the valve of 150 mm in diameter. However, pressure values are greater in the case 300 mm due to the bigger size of the valve. The minimum value of stagnation point also appears at $0°$ position, causing the lowest pressure loss here. However, the exact value of the pressure can be read from color chart on the left of the picture..

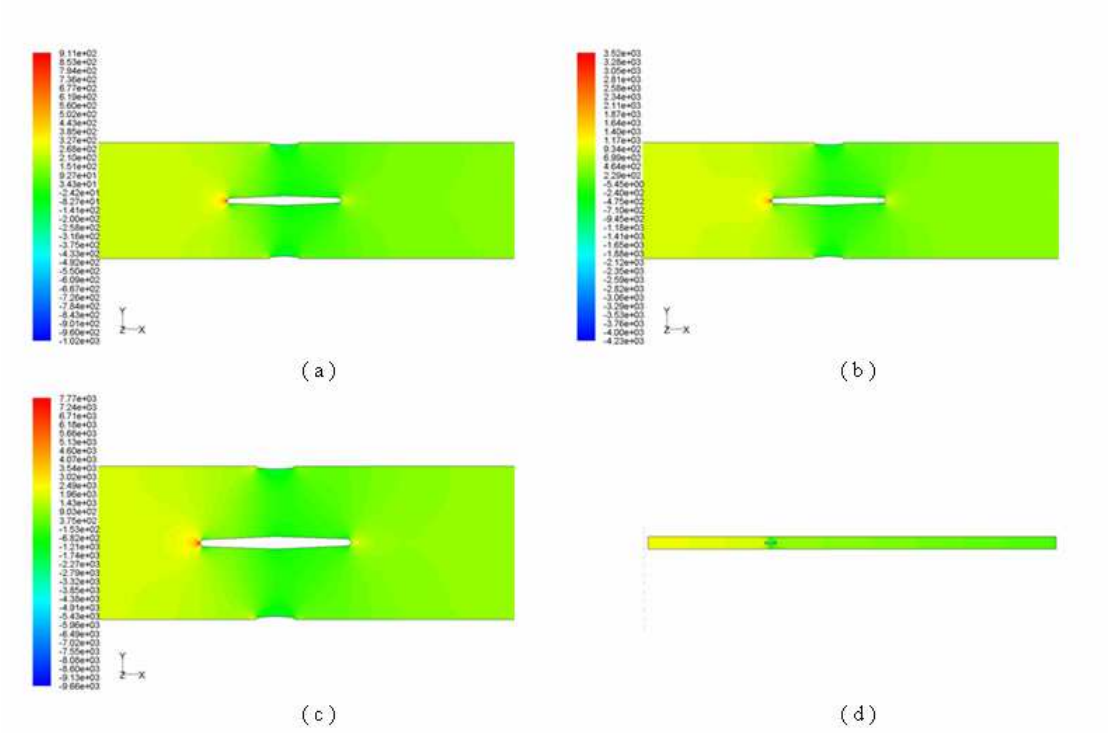

Figure 4.6 : The pressure distribution of the flow at $0°$ position of the 300 mm valve at velocity inlet of (a) $1m/s$, (b) $2m/s$, (c) $3m/s$ and (d) $3m/s$ (large view)

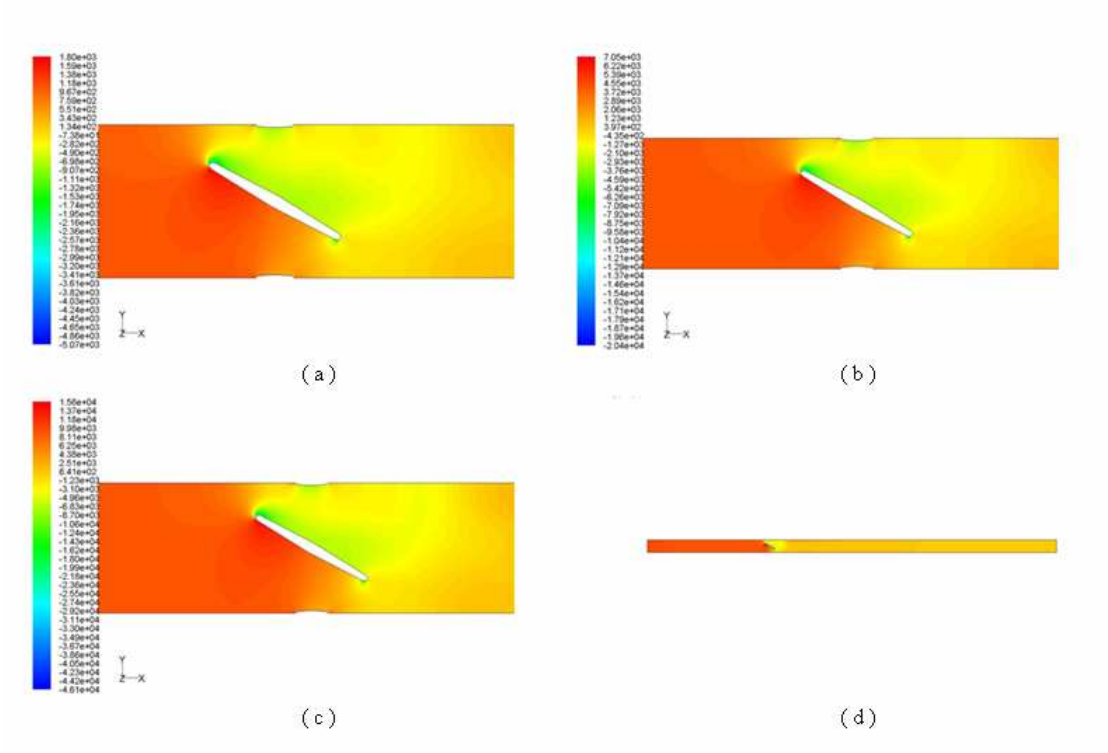

Figure 4.7 : The pressure distribution of the flow at $30°$ position of the 300 mm valve at velocity inlet of (a) $1m/s$, (b) $2m/s$, (c) $3m/s$ and (d) $3m/s$ (large view)

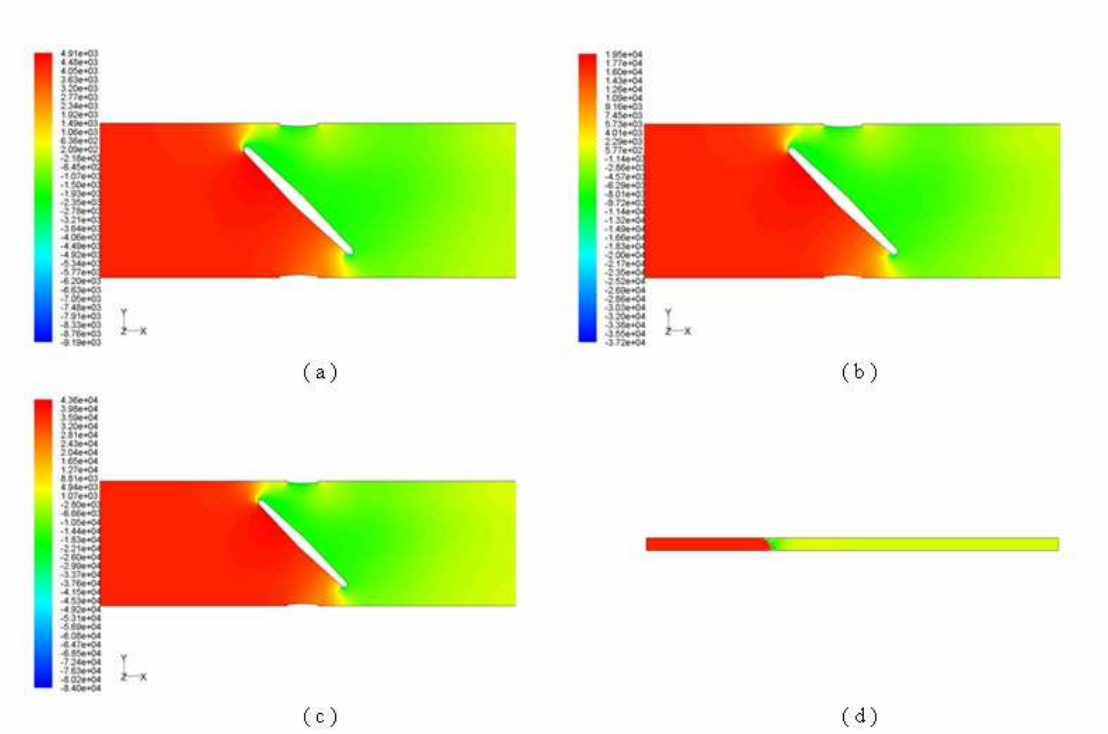

Figure 4.8 : The pressure distribution of the flow at $45°$ position of the 300 mm valve at velocity inlet of (a) $1m/s$, (b) $2m/s$, (c) $3m/s$ and (d) $3m/s$ (large view)

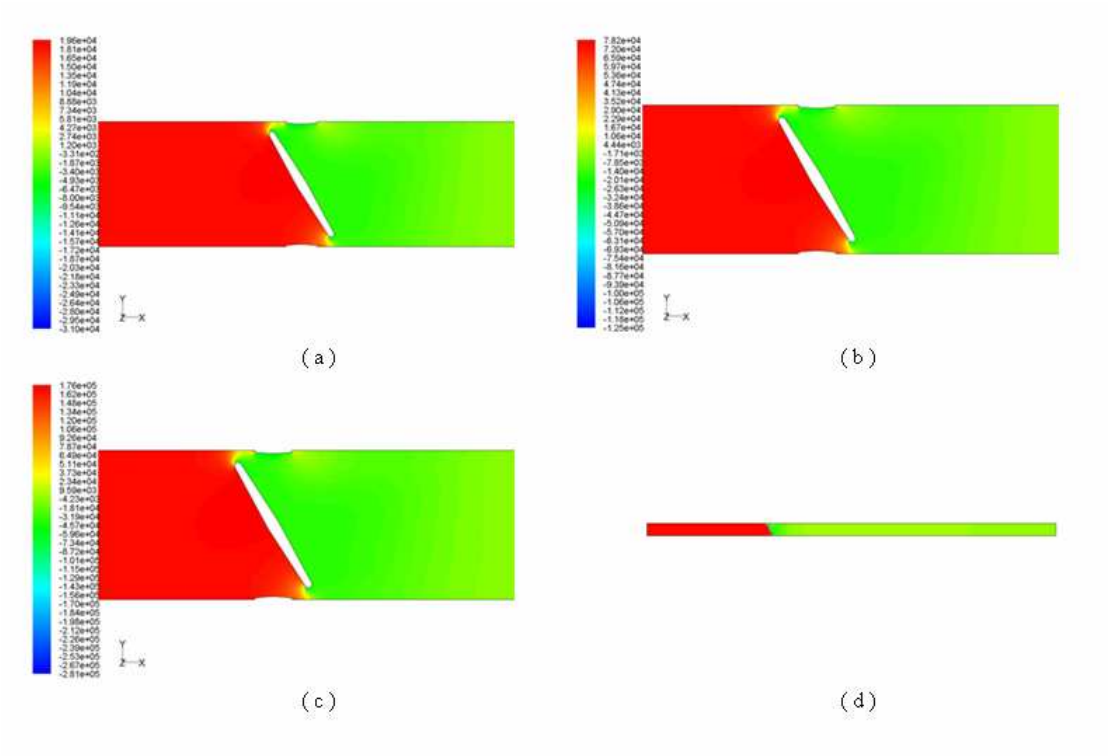

Figure 4.9 : The pressure distribution of the flow at $60°$ position of the 300 mm valve at velocity inlet of (a) $1m/s$, (b) $2m/s$, (c) $3m/s$ and (d) $3m/s$ (large view)

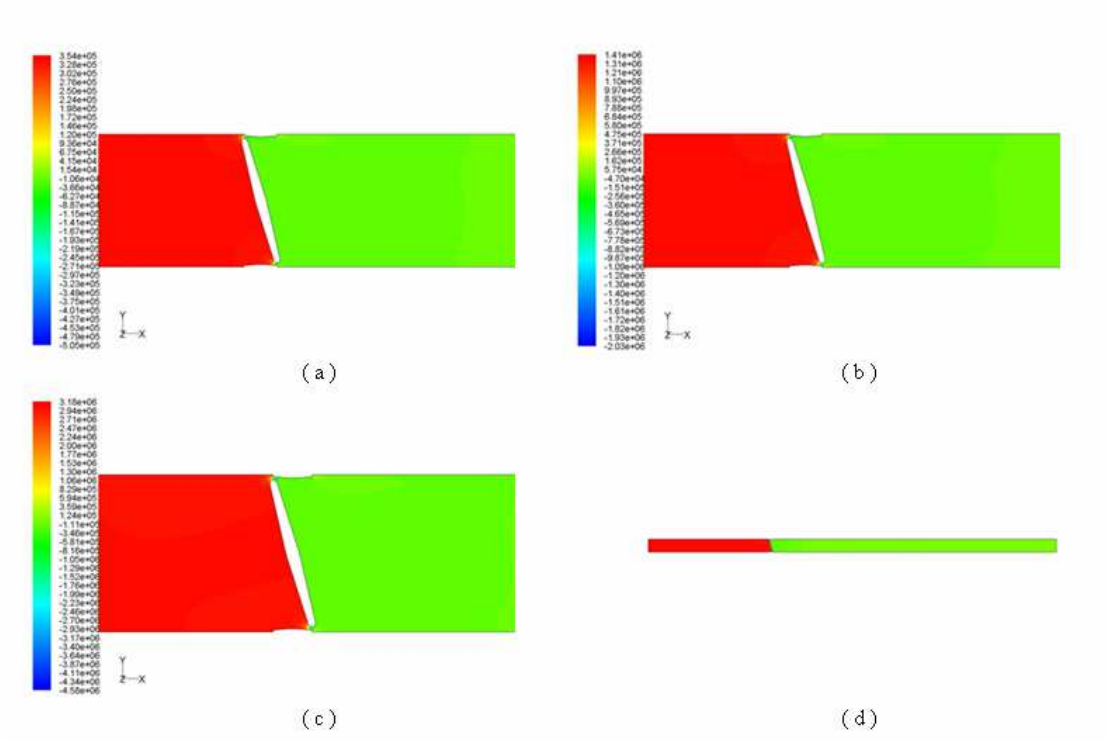

Figure 4.10 : The pressure distribution of the flow at $75°$ position of the 300 mm valve at velocity inlet of (a) $1m/s$, (b) $2m/s$, (c) $3m/s$ and (d) $3m/s$ (large view)

4.2. The Velocity Distribution

The velocity distributions, in this part will be represented by velocity vectors. This help to display the velocity value and direction of the fluid around the valve. Fig 4.11-4.15 show the velocity distribution of fluid around the butterfly valve for diameter of 150 mm. They were found that the velocity values are proportional to the mass flow rate. The high gradient of fluid velocity appears around the tip of the butterfly valve due to the change of valve curve. Also in almost closed position, the velocity value becomes high between the pipe surface and the butterfly valve. The velocity will be increased if the flow area is smaller as shown below.

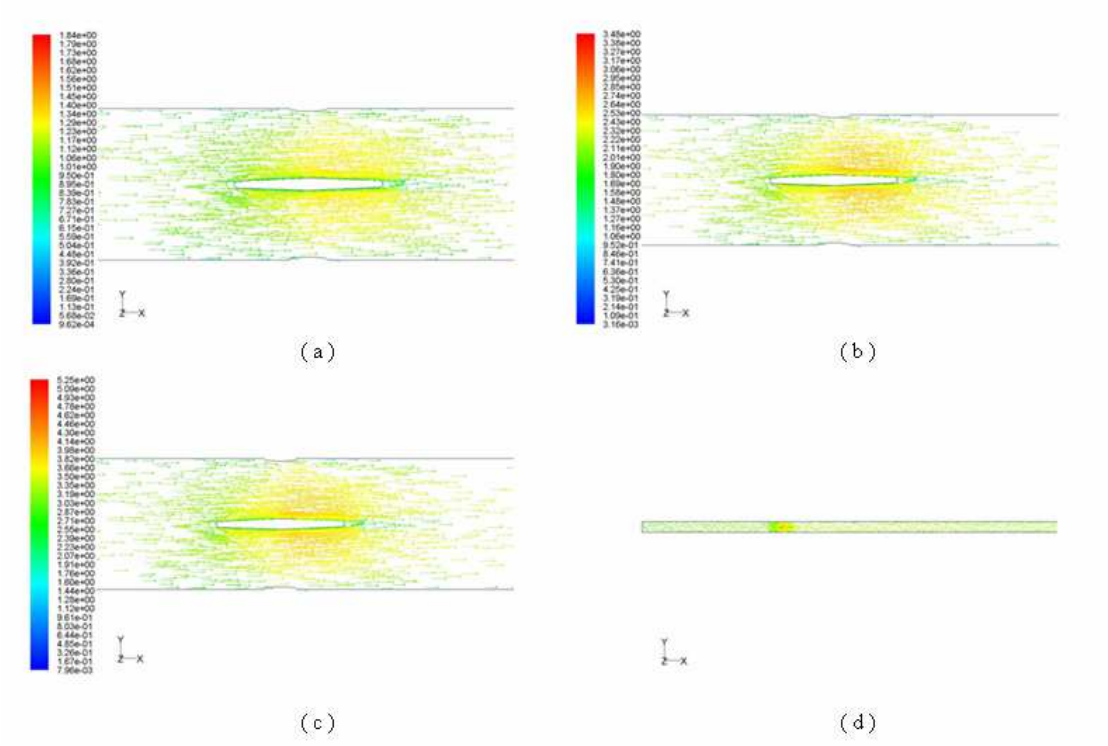

Figure 4.11 : The velocity distribution of the flow at $0°$ position of the 150 mm valve at velocity inlet of (a) $1m/s$, (b) $2m/s$, (c) $3m/s$ and (d) $3m/s$ (large view)

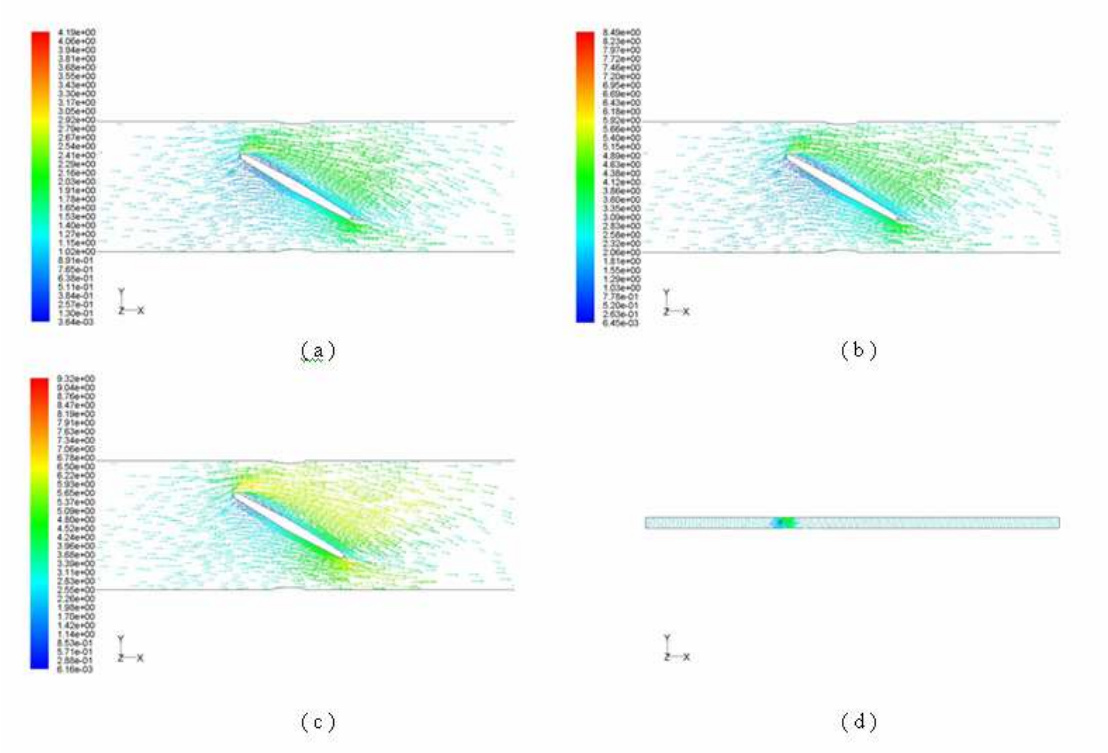

Figure 4.12 : The velocity distribution of the flow at $30°$ position of the 150 mm valve at velocity inlet of (a) $1m/s$, (b) $2m/s$, (c) $3m/s$ and (d) $3m/s$ (large view)

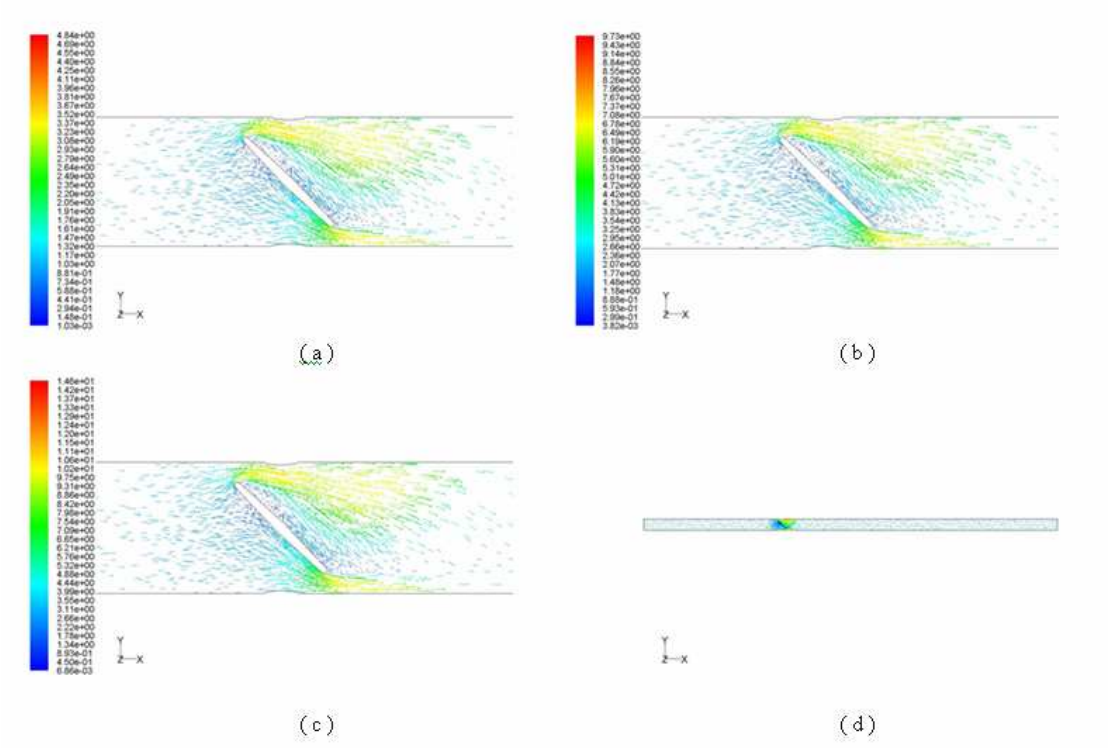

Figure 4.13 : The velocity distribution of the flow at $45°$ position of the 150 mm valve at velocity inlet of (a) $1m/s$, (b) $2m/s$, (c) $3m/s$ and (d) $3m/s$ (large view)

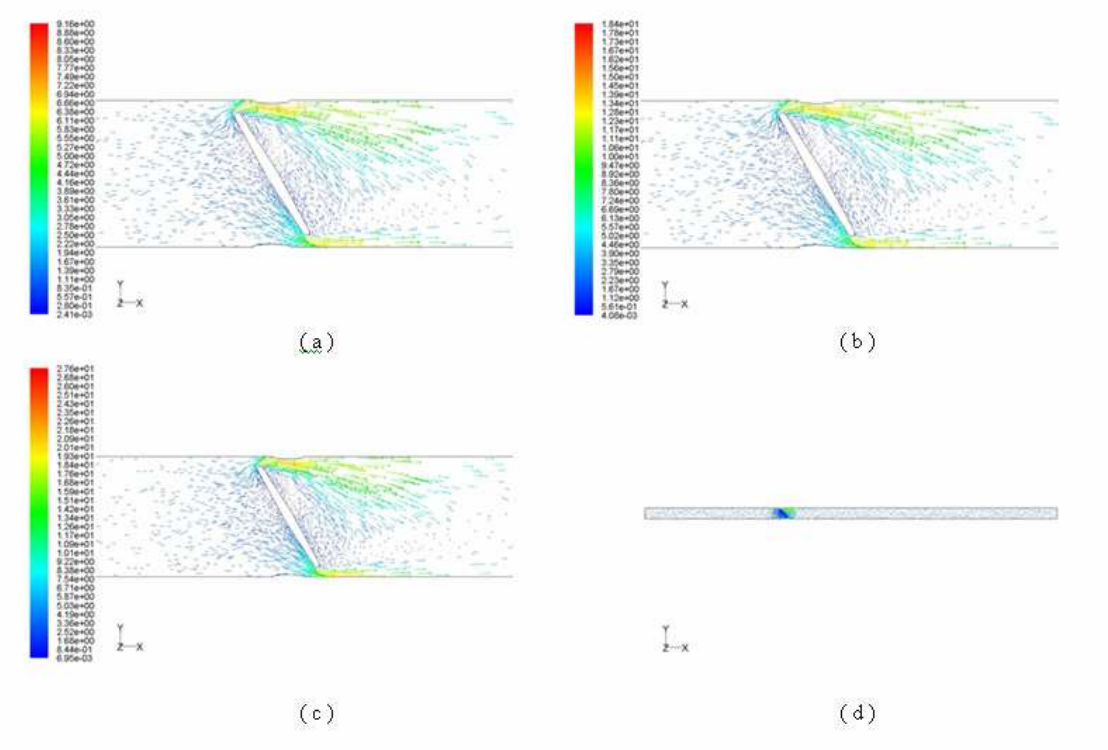

Figure 4.14 : The velocity distribution of the flow at $60°$ position of the 150 mm valve at velocity inlet of (a) $1 m/s$, (b) $2 m/s$, (c) $3 m/s$ and (d) $3 m/s$ (large view)

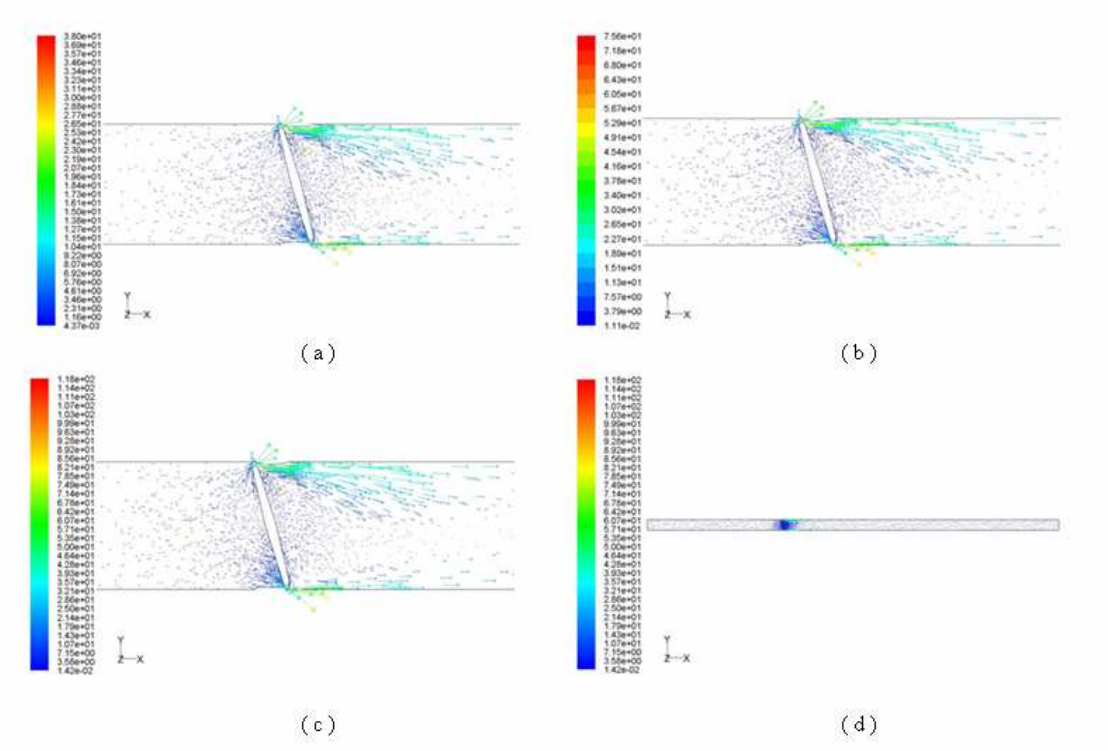

Figure 4.15 : The velocity distribution of the flow at $75°$ position of the 150 mm valve at velocity inlet of (a) $1 m/s$, (b) $2 m/s$, (c) $3 m/s$ and (d) $3 m/s$ (large view)

For butterfly valve of 300 mm in diameter, the flow-fields are slightly different than for the valve of 150 mm in diameter. Fig 4.16-4.20 show the value and direction of velocity vector of the flow at 5 positions of the valve under 3 flow-rates. It was found that the flow did not follow and stuck the valve's surface at position of $45°$. It caused a small bubble behind the valve's disk and became bigger in position of $60°$. It's also found that the flow around the valve, in position of $75°$, showed high turbulent condition behind the butterfly valve due to the smaller section area of the flow.

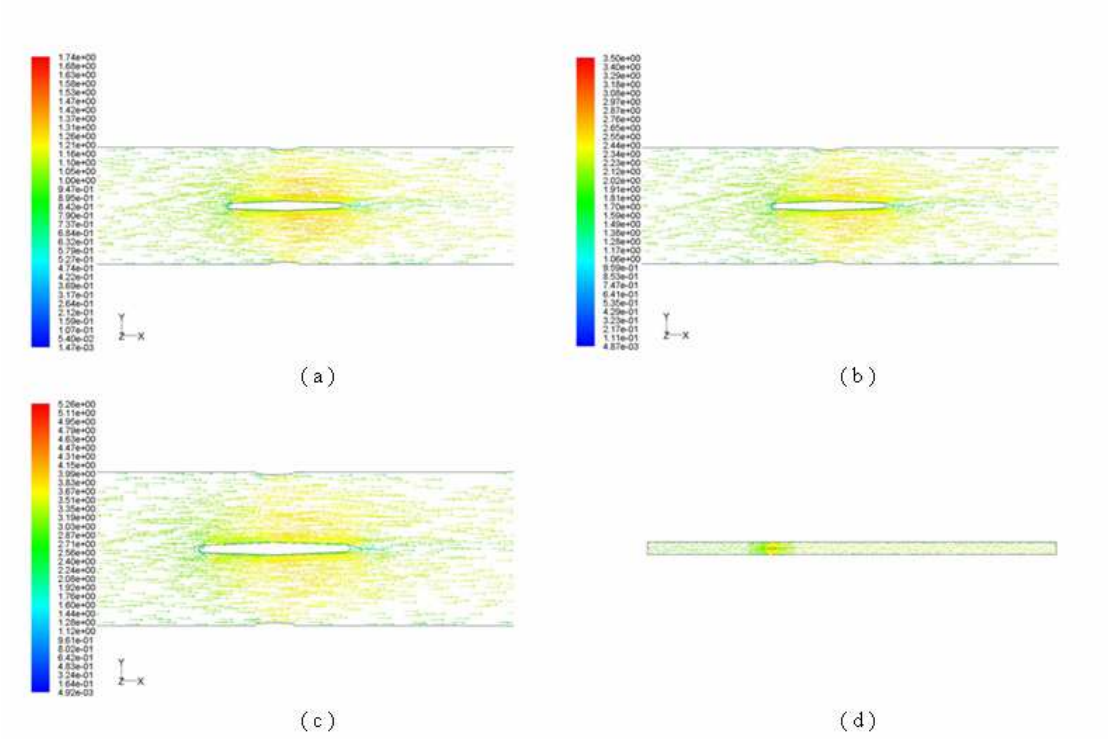

Figure 4.16 : The velocity distribution of the flow at $0°$ position of the 300 mm valve at velocity inlet of (a) $1m/s$, (b) $2m/s$, (c) $3m/s$ and (d) $3m/s$ (large view)

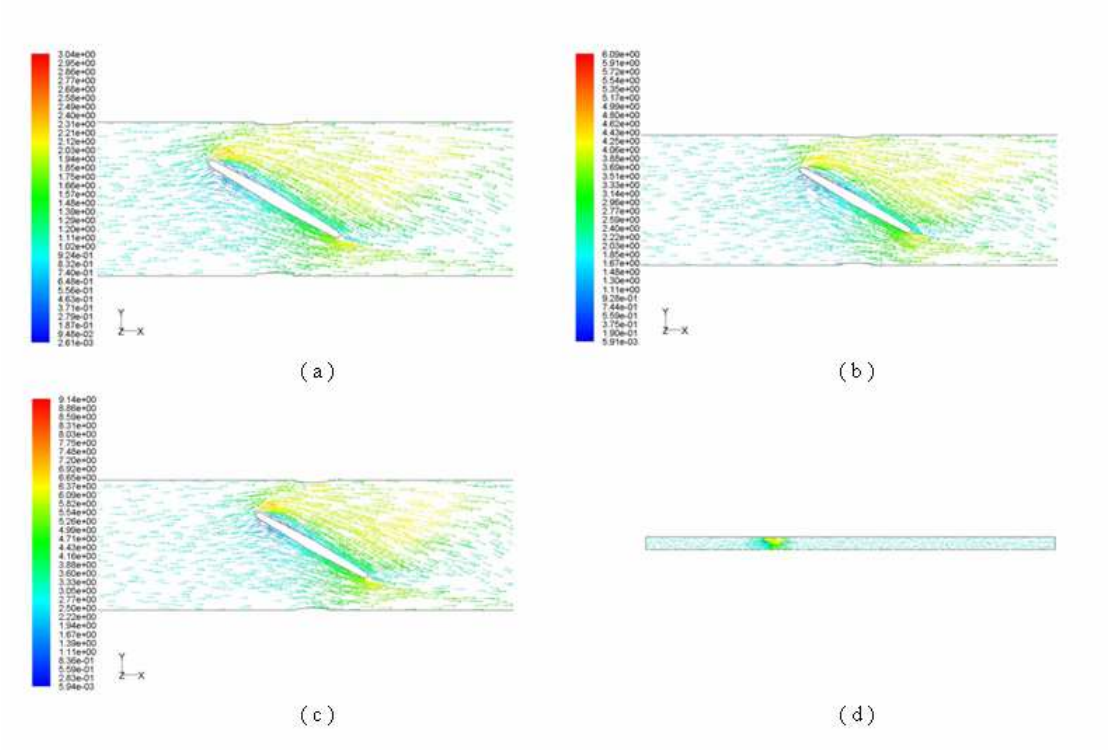

Figure 4.17 : The velocity distribution of the flow at $30°$ position of the 300 mm valve at velocity inlet of (a) $1m/s$, (b) $2m/s$, (c) $3m/s$ and (d) $3m/s$ (large view)

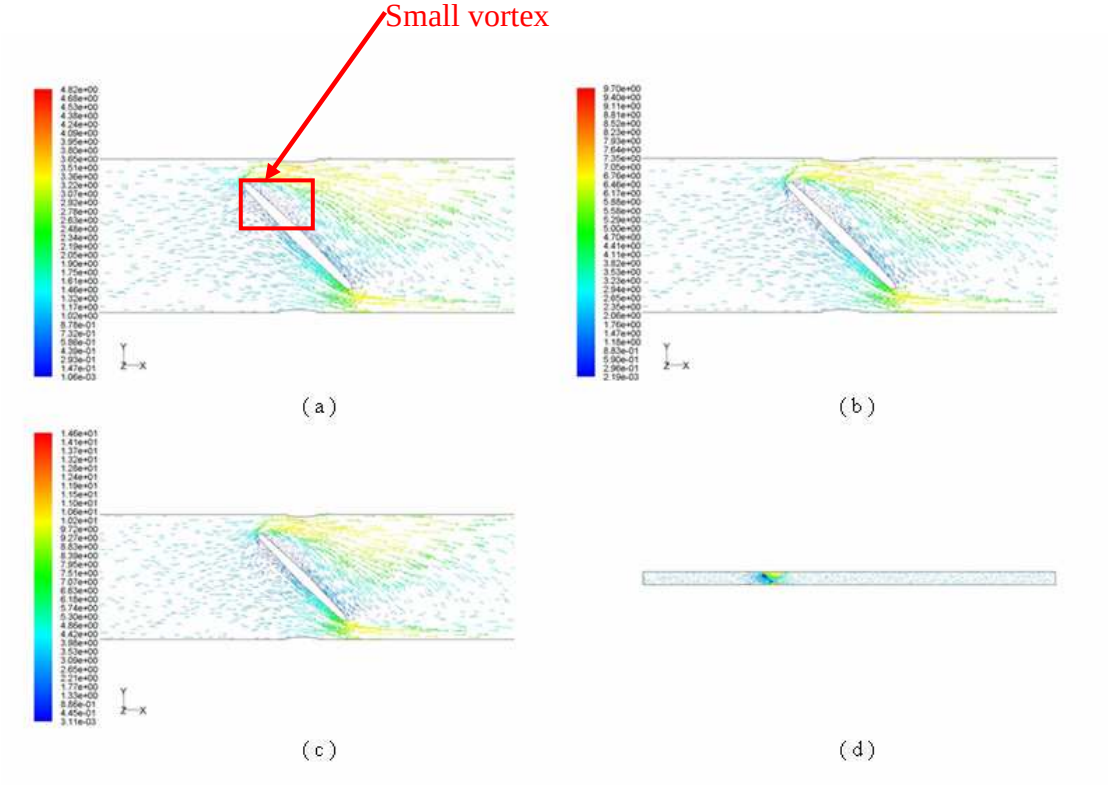

Figure 4.18 : The velocity distribution of the flow at $45°$ position of the 300 mm valve at velocity inlet of (a) $1m/s$, (b) $2m/s$, (c) $3m/s$ and (d) $3m/s$ (large view)

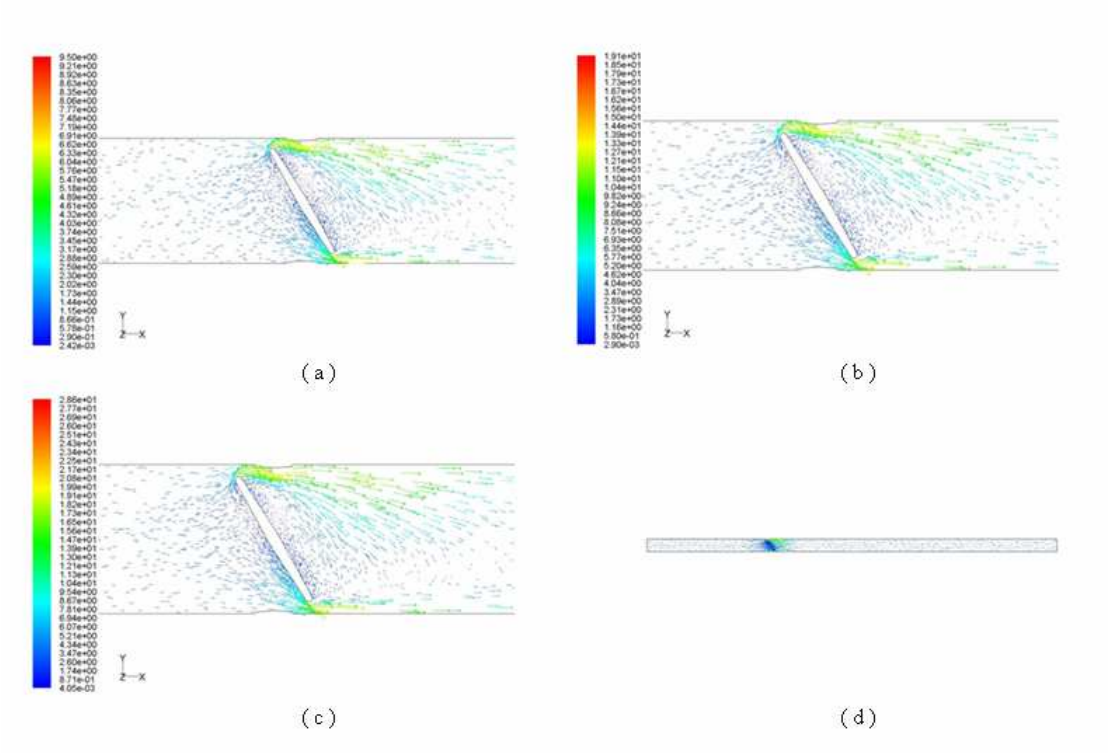

Figure 4.19 : The velocity distribution of the flow at $60°$ position of the 300 mm valve at velocity inlet of (a) $1m/s$, (b) $2m/s$, (c) $3m/s$ and (d) $3m/s$ (large view)

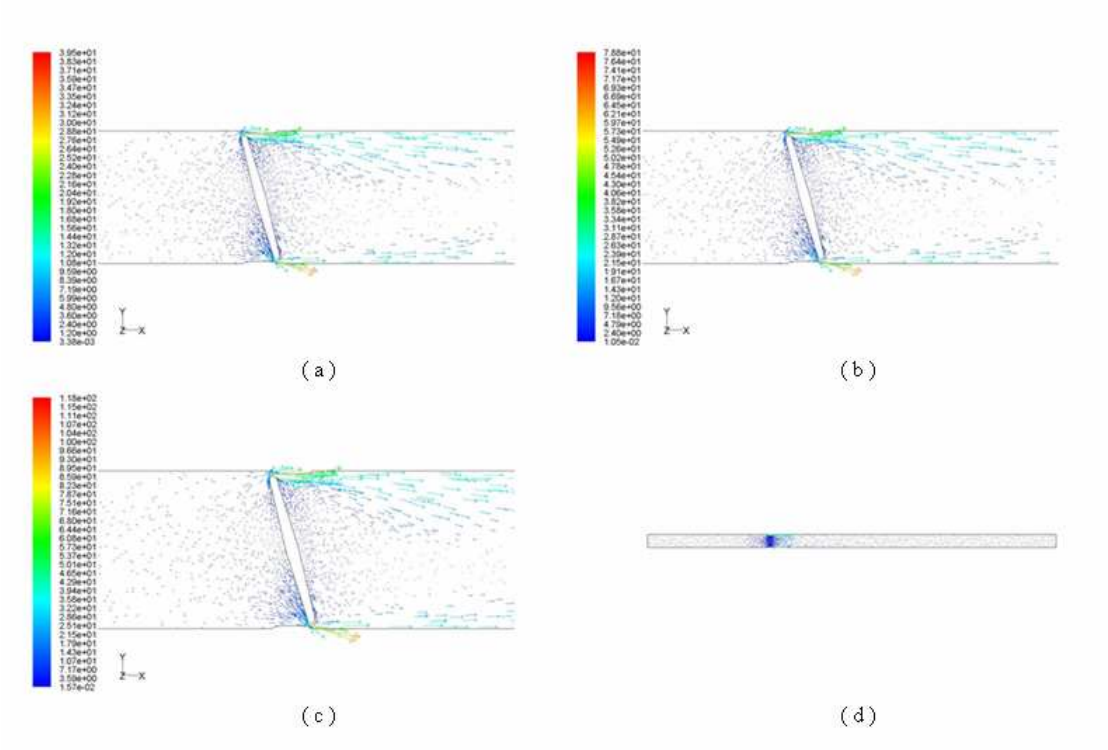

Figure 4.20 : The velocity distribution of the flow at $75°$ position of the 300 mm valve at velocity inlet of (a) $1m/s$, (b) $2m/s$, (c) $3m/s$ and (d) $3m/s$ (large view)

The top views of the water flow in horizontal plane are shown in Fig 4.21. They show that when the water flows past the valve in different positions, the flow characteristics change. The vortex was found near the left-right tips of the butterfly valve which was caused by the holes of the motor shaft. By increasing the angle of the valve, the vortex became bigger in every degree of increasing. For the position of $75°$, it was found that the vortex was the biggest and the velocity value was low in the horizontal plane.

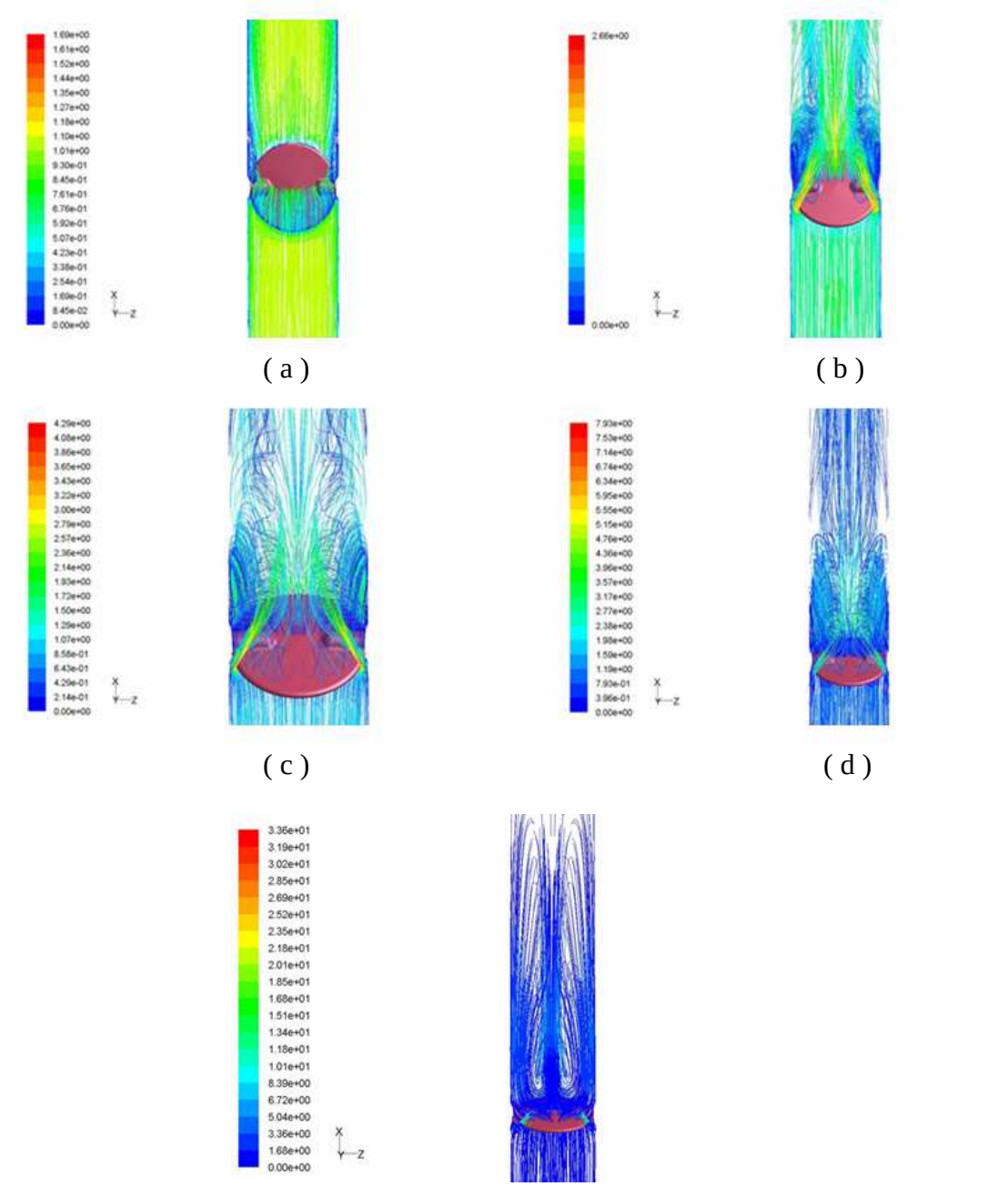

(a) (b) (c) (d) (e)

Figure 4.21 : The velocity distribution of the water flow on top view at velocity inlet of $1 m/s$ of (a) $0°$, (b) $30°$, (c) $45°$, (d) $60°$ and (e) $75°$ position

4.3. Characteristic of Loss Coefficient

4.3.1 Loss Coefficient of Static Analysis

The values of pressure drop across the butterfly valve were investigated using commercial fluid dynamics software FLUENT. They were calculated in order to compute the dimensionless value of loss coefficient, K. The table 4.1 and 4.2 show the value of loss coefficient of the 150 and 300 mm butterfly valve, respectively. They were found that the K values are independent of flow rate but that they are affected by changing position of the valve's disk. By increasing valve disk's angle, the value of loss coefficient becomes greater.

Position	*Velocity*(m/s)	$P_{in}(Pa)$	$P_{out}(Pa)$	$\Delta P(Pa)$	K
0°	1	291.125	163.443	127.682	0.255364
	2	1046.423	565.492	480.931	0.2404655
	3	2223.419	1173.931	1049.488	0.233219556
30°	1	1155.322	199.092	956.23	1.91246
	2	4470.506	709.659	3760.847	1.8804235
	3	9903.753	1485.919	8417.834	1.870629778
45°	1	4168.2026	201.481	3966.7216	7.9334432
	2	16462.705	702.004	15760.701	7.8803505
	3	36753.918	1463.191	35290.727	7.842383778
60°	1	19038.566	186.983	18851.583	37.703166
	2	75754.367	644.659	75109.708	37.554854
	3	169902.03	1335.313	168566.717	37.45927044
75°	1	342717.81	-192.15337	342909.9634	685.8199267
	2	1365400	-939.139	1366339.139	683.1695695
	3	3064062.8	-2195.345	3066258.145	681.3906989

Table 4.1 : The values of pressure drop and the loss coefficient of the flow past the 150 mm butterfly valve in 5 positions under $1m/s$, $2m/s$ and $3m/s$ inlet conditions

Position	*Velocity*(m/s)	$P_{in}(Pa)$	$P_{out}(Pa)$	$\Delta P(Pa)$	K
0°	1	252.52713	109.20542	143.32171	0.28664342
	2	913.25879	381.87393	531.38486	0.26569243
	3	1940.7196	797.73444	1142.98516	0.253996702
30°	1	1068.0927	135.1205	932.9722	1.8659444
	2	4142.7285	471.34937	3671.37913	1.835689565
	3	9053.3037	996.25732	8057.04638	1.790454751
45°	1	4266.8779	133.56094	4133.31696	8.26663392
	2	16912.287	472.07385	16440.21315	8.220106575
	3	37889.979	987.18365	36902.79535	8.200621189
60°	1	19021.906	128.36682	18893.53918	37.78707836
	2	75804.75	449.65567	75355.09433	37.67754717
	3	170266.64	939.26953	169327.3705	37.62830455
75°	1	337277.53	45.769901	337231.7601	674.4635202
	2	1346350.9	98.651268	1346252.249	673.1261244
	3	3023281.8	119.77937	3023162.021	671.8137824

Table 4.2 : The values of pressure drop and the loss coefficient of the flow past the 300 mm butterfly valve in 5 positions under $1m/s$, $2m/s$ and $3m/s$ inlet conditions

The values in Table 4.1 and 4.2 can obviously show in linear graph pattern. Fig 4.22 and Fig 4.23 show the K values of the valve of 150 and 300 mm, respectively which vary from $0°$ to $75°$. It was also found that the loss coefficient is independent on the condition at the inlet but dependent on the geometry of the butterfly valve.

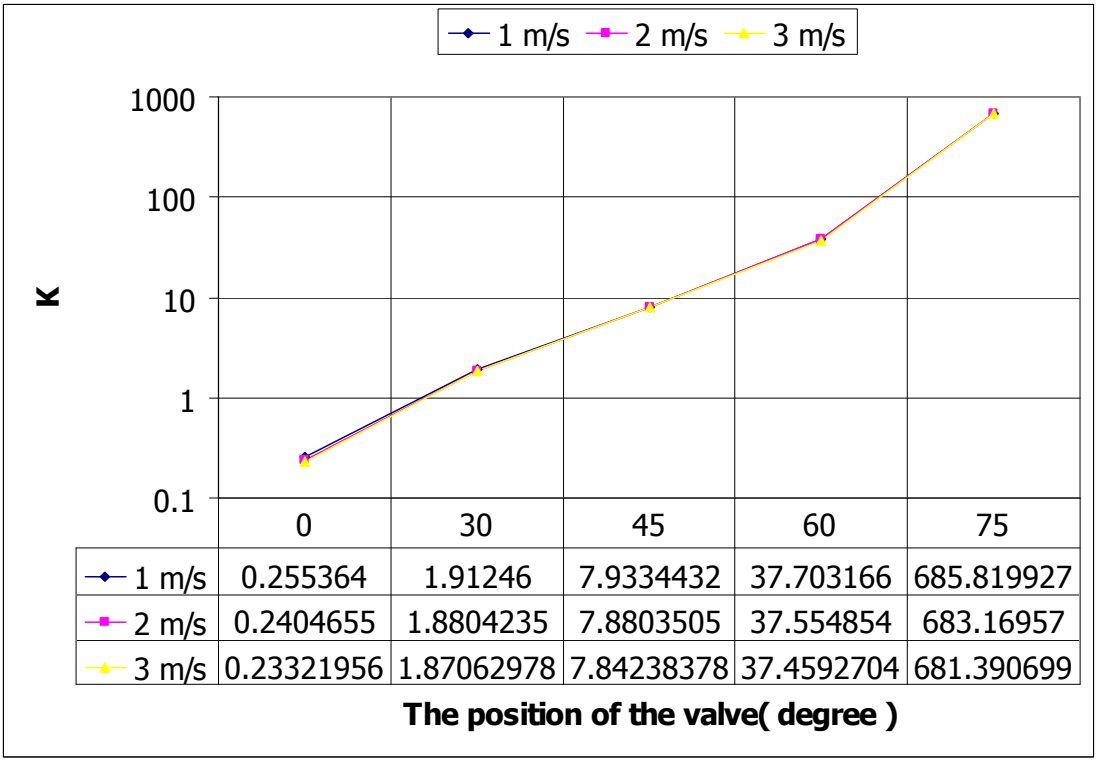

Figure 4.22 : The characteristic of the loss coefficient in 5 positions of the 150 mm butterfly valve under $1 m/s$, $2 m/s$ and $3 m/s$ inlet conditions

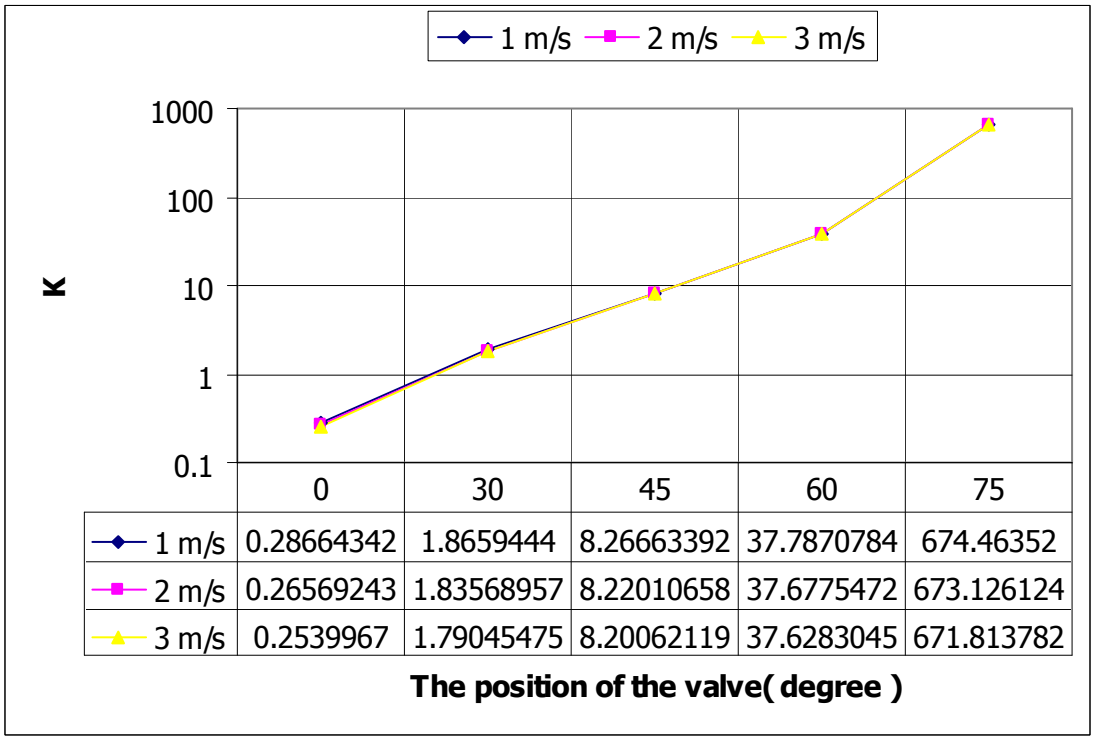

Figure 4.23 : The characteristic of the loss coefficient in 5 positions of the 300 mm butterfly valve under $1 m/s$, $2 m/s$ and $3 m/s$ inlet conditions

4.3.2 Loss Coefficient of Dynamic Analysis

Fig 4.24 shows the value of loss coefficient from $0°$ to $90°$ position of 150 mm valve disk in dynamic analysis. When the velocity at the inlet of the flow is equal to 1 m/s, it was found that the K value is proportional to the disk's position. By increasing the angle of the disk, the K value becomes greater until it reaches 262.8 at $82.5°$. Due to "no-flow" condition, the value of loss coefficient is infinity at $90°$ position(completely closed)

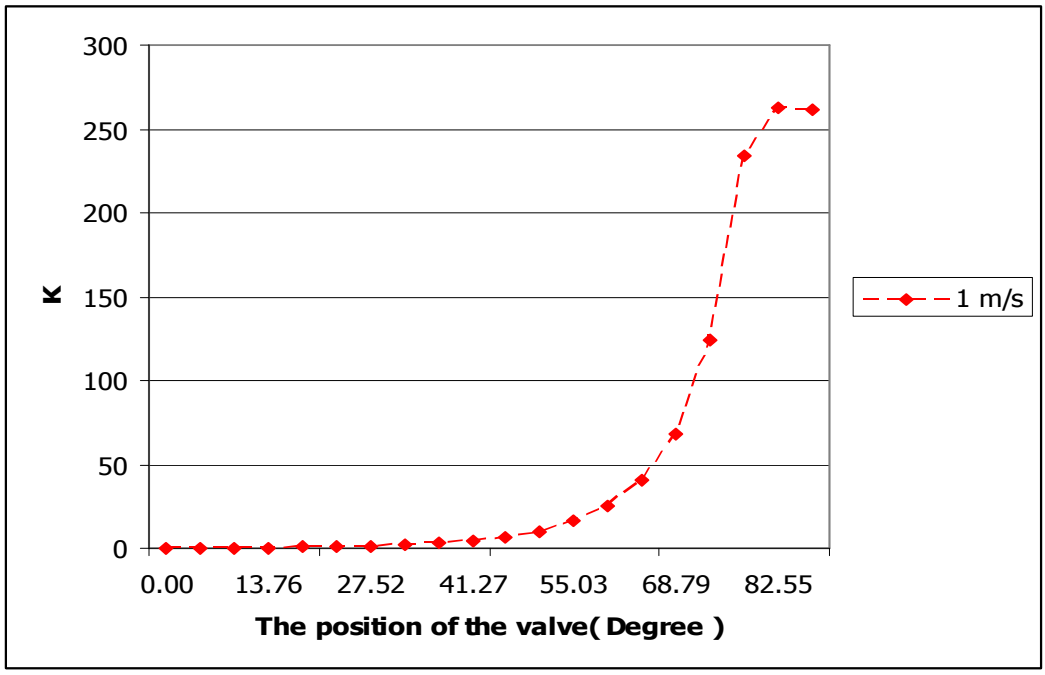

Figure 4.24 : The characteristic of loss coefficient from $0°$ to $90°$ position of the 150 mm butterfly valve under $1 m/s$ inlet condition.

The values of loss coefficient from $90°$ to $180°$ position of 150 mm valve disk in dynamic analysis are shown in Fig 4.25. It was found that when the valve is opened, the K value remains constant around 262 in $10°$(from completely closed position). Also, it was found that at $0°$ or $180°$ the lost coefficient is minimum so that the flow rate is maximum.

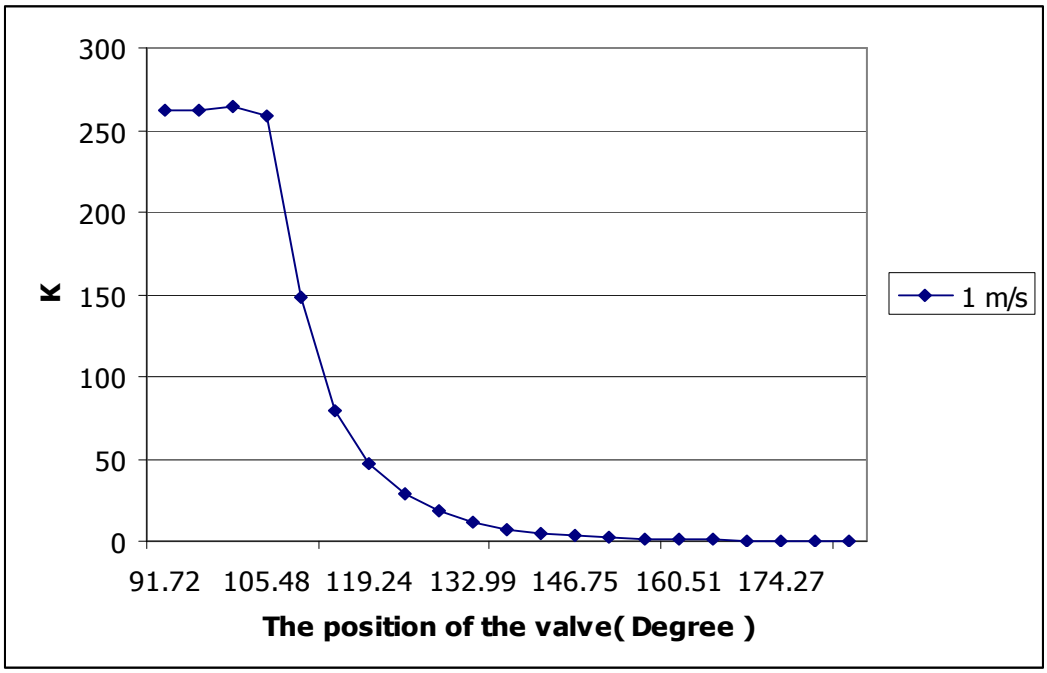

Figure 4.25 : The characteristic of loss coefficient from $90°$ to $180°$ position of the 150 mm butterfly valve under $1 m/s$ inlet condition.

For 300 mm valve disk, the comparison was made between normally closed(40 seconds for closing) and rapidly closed(1 seconds for closing) conditions. Fig 4.26 shows that values of K present slightly different trend for the 2 conditions. The K value becomes bigger when the degree of valve disk increases. The maximum value of loss coefficient is 265.77 at $77°$ position for rapidly closed condition. It is not different with normally closed condition, which has the maximum value of loss coefficient of 261.3 at $87.13°$ position. Similar to 150 mm valve, the K values remain constant when the valve is almost closed. And it reaches infinity when the valve is completely closed. Same as the closing turn, the normally and rapidly opened conditions are slightly different as shown in Fig 4.27. The maximum value of K occurs at the same point, the $91.72°$ valve position. The values are 262.25 and 278.12 for normally and rapidly opened conditions, respectively.

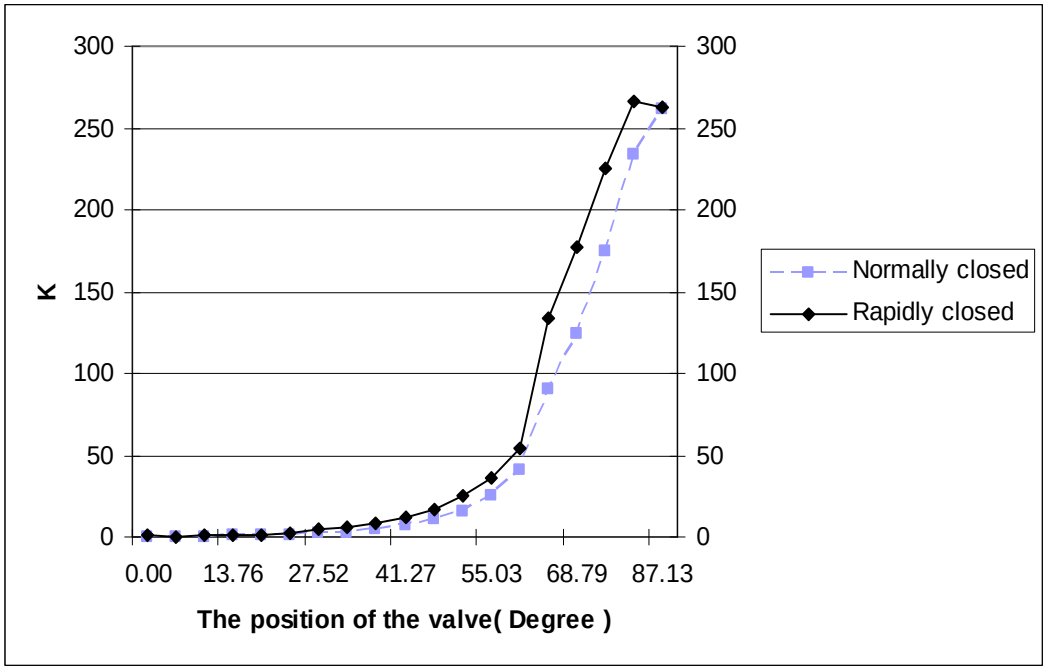

Figure 4.26 : The comparison between the characteristic of loss coefficient of normally and rapidly closed condition from $0°$ to $90°$ position of the 300 mm butterfly valve under $1 m/s$ inlet condition.

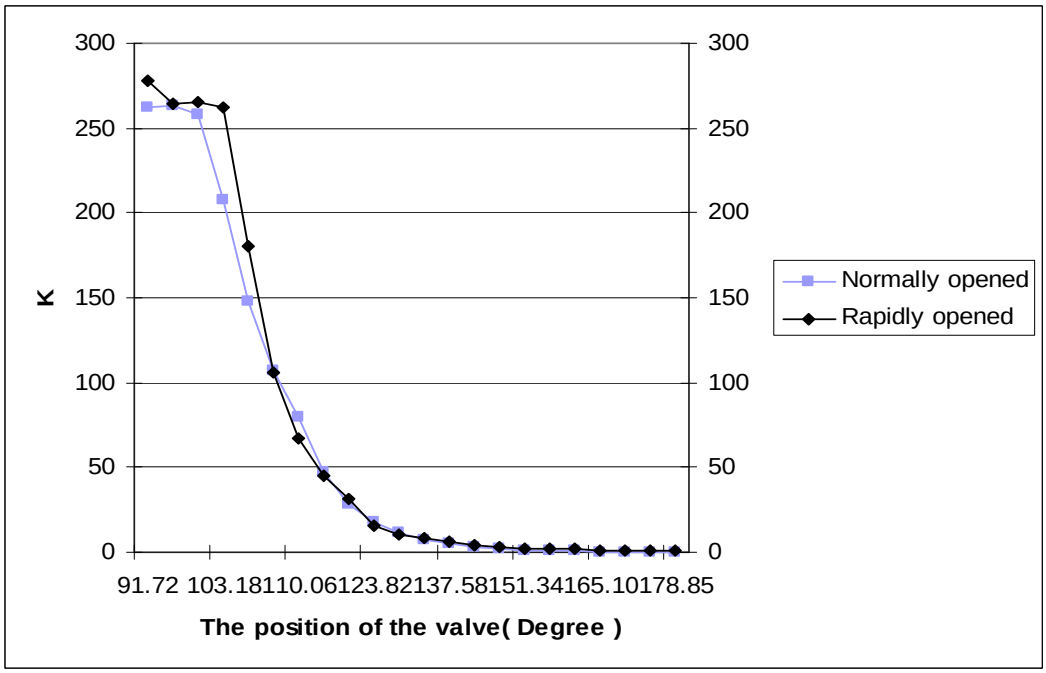

Figure 4.27 : The comparison of the characteristic of loss coefficient between normally and rapidly opened condition from $90°$ to $180°$ position of the 300 mm butterfly valve under $1 m/s$ inlet condition.

4.4. The Characteristic of Torque

4.4.1 Torque Characteristic of Static Analysis

The characteristic of torque, used to rotate the valve disk was investigated in 5 positions of the valve, consisting of $0°$, $30°$, $45°$, $60°$ and $75°$. The velocity inlet was set to value equal to 1, 2 and 3 m/s. We compare the torque characteristic between the valve of 150 and 300 mm; results are shown in Fig 4.28. It was found that torque value of 300 mm valve is greater than 150 mm because the fluid force distributes on the bigger integral area of the butterfly valve. By increasing the velocity at the inlet, torque value, used to move the disk position becomes bigger. And it's also bigger when the area of the flow is decreased. The value of the torque can be read directly below.

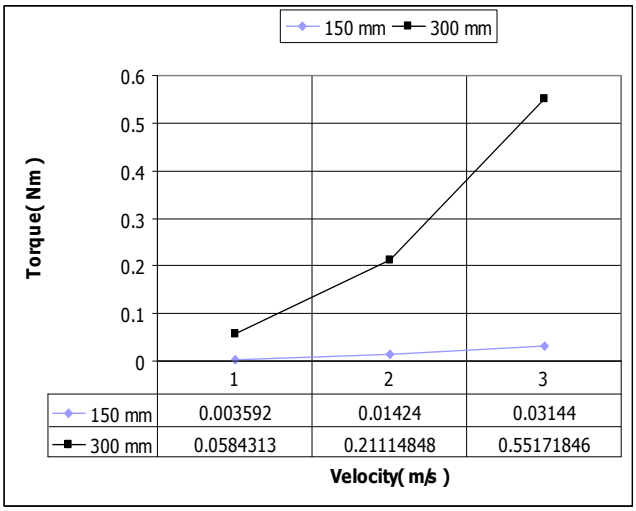

(a)

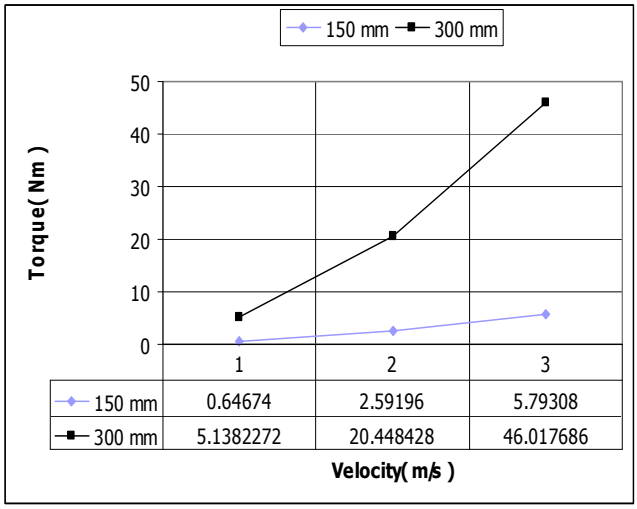

(b)

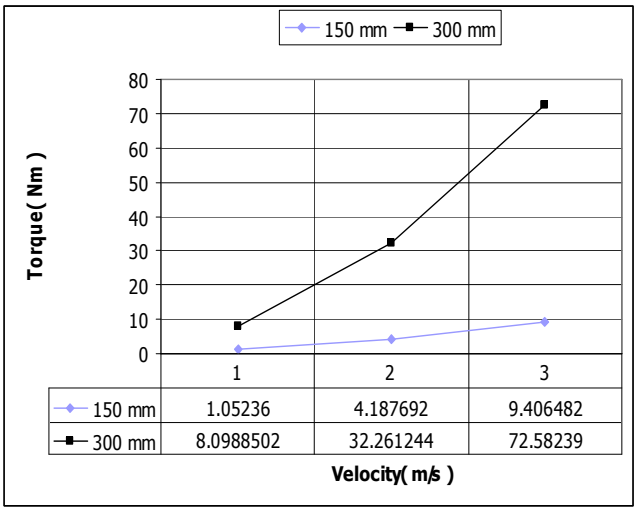

(c)

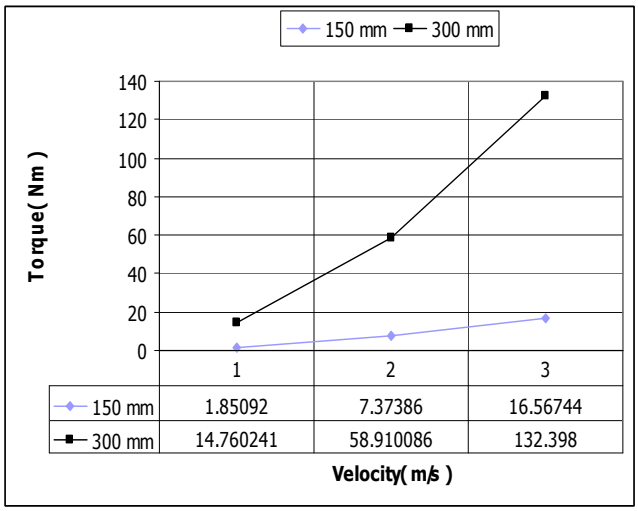

(d)

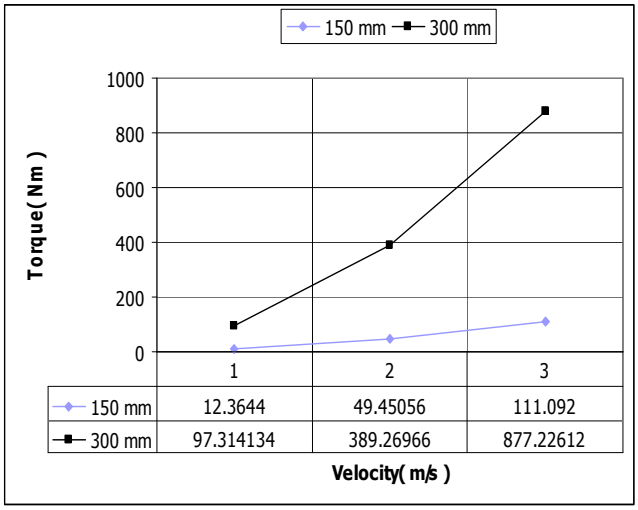

(e)

Figure 4.28 : The comparison of torque characteristic between the 150 and 300 mm butterfly valve of (a) 0°, (b) 30°, (c) 45°, (d) 60° and (e) 75° position

4.4.2 Torque Characteristic of Dynamic Analysis

The torque behavior was measured from $0°$ to $180°$ of 150 mm valve disk at velocity of $1\,m/s$. It was found that the maximum torque in the closing turn is 2.5 Nm, which occurs at $73.4°$. For the opening turn the maximum torque is -2.88 Nm, which is slightly greater than the closed turn as shown in Fig 4.29; this maximum value is reached at $20°$ However, the value of torque around $90°$ of valve position is not valid due to the limit of the commercial program.

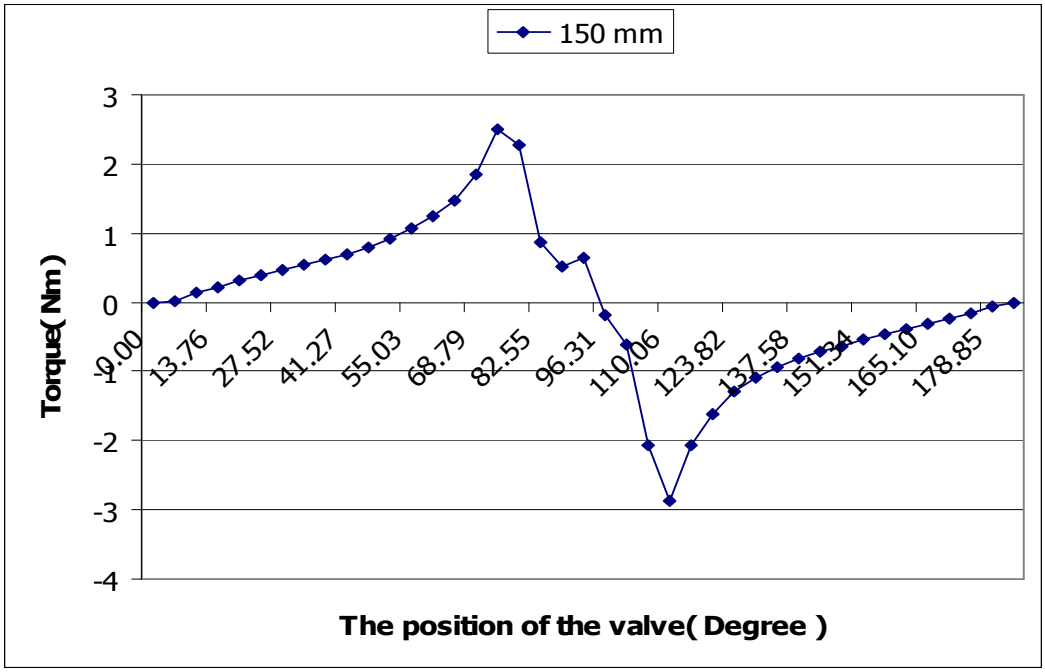

Figure 4.29 : The torque characteristic from $0°$ to $180°$ position of the 150 mm butterfly valve under $1 m/s$ inlet condition.

When the comparison between normally rotated (40 seconds for $90°$) and rapidly rotated(1 seconds for $90°$) was made, it is found that the torque values for the two cases are no much different as illustrated in Fig 4.30. The maximum values of torque in the closing turn are 19.3 and 21.2 Nm, which occurs at $69°$ and $73°$, for normally and rapidly closed conditions, respectively. For opening condition, the maximum torque values are 22.5 and 23.3 Nm, at $105°$ and $106°$, for normally and rapidly closed conditions, respectively. The value of torque around $90°$ is also not valid in this case. The exact value can be read below.

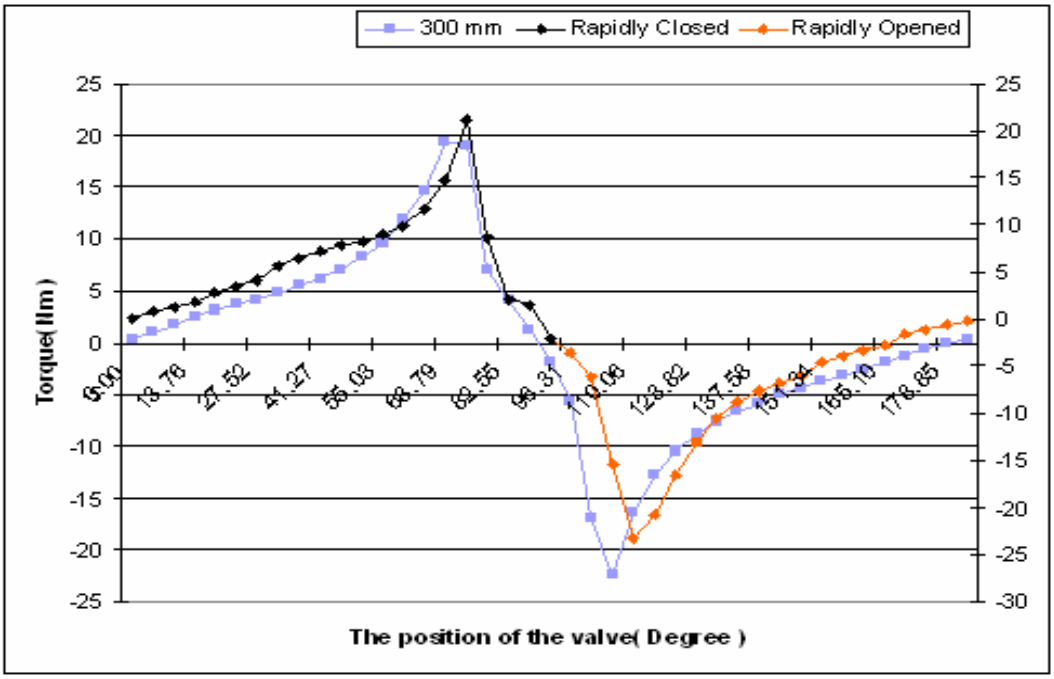

Figure 4.30 : The comparison of the characteristic of loss coefficient between normally and rapidly rotated condition from $0°$ to $180°$ position of the 300 mm butterfly valve under $1 m/s$ inlet condition.

4.5. The Experimental Results

From the experiment of the 150 mm butterfly valve, it was found that the loss coefficient is around 6.1 in average for $45°$, 33.97 for $60°$ and 1225.6 for $75°$ as shown in Table 4.3. And the torque values also reach the maximum at $75°$. The errors occur in the experimental results in K and torque values. For the loss coefficient, it was found that K is not constant in each position of the butterfly valve. The cause of these errors may be due to the flow in the pipe that is highly turbulent, thus inducing strong pressure fluctuations. Also, measurements show that the torque of $60°$ valve position is smaller than the torque of $45°$ valve position while it should be greater. The cause of this problem was clearly known by the device. The range of torque-meter is 0-2000 Nm, which is huge for the range of torque values measured in this experiment so that errors can be large.

Position	*State*	$\dot{V}(L/s)$	K	$Torque(N \cdot m)$
45°	1	13.2888	3.996953394	0.412
	2	19.656	6.60786	0.698
	3	25.753	7.697278107	1.148
60°	1	13.418	34.38040657	0.0512
	2	19.796	37.1388	0.3892
	3	25.51	30.37814911	0.91
75°	1	10.147	1245.764168	2.3241
	2	13.5	1232.120502	2.532
	3	16.675	1198.889024	3.0777

Table 4.3 : The experimental results of the flow past the butter valve at 45°, 60° and 75° under 3 inlet conditions

The K results between experimental and numerical studies were compared at 45°, 60° and 75° under 3 load states as shown in Fig 4.31. In every load conditions, the loss coefficient values computed by numerical method are constant at the same valve position. The most differences between experimental and numerical results are estimated to 50% and 20% for 45° and 60°, respectively. Conversely, the minimum differences show only 3.5% and 1.7% for 45° and 60°, respectively. However, there is a big error in the comparison of the 75° valve position. It may be caused by both experimental and numerical part. Because the flow inside the pipe at 75° is really complex, the calculation by numerical method may be erroneous.

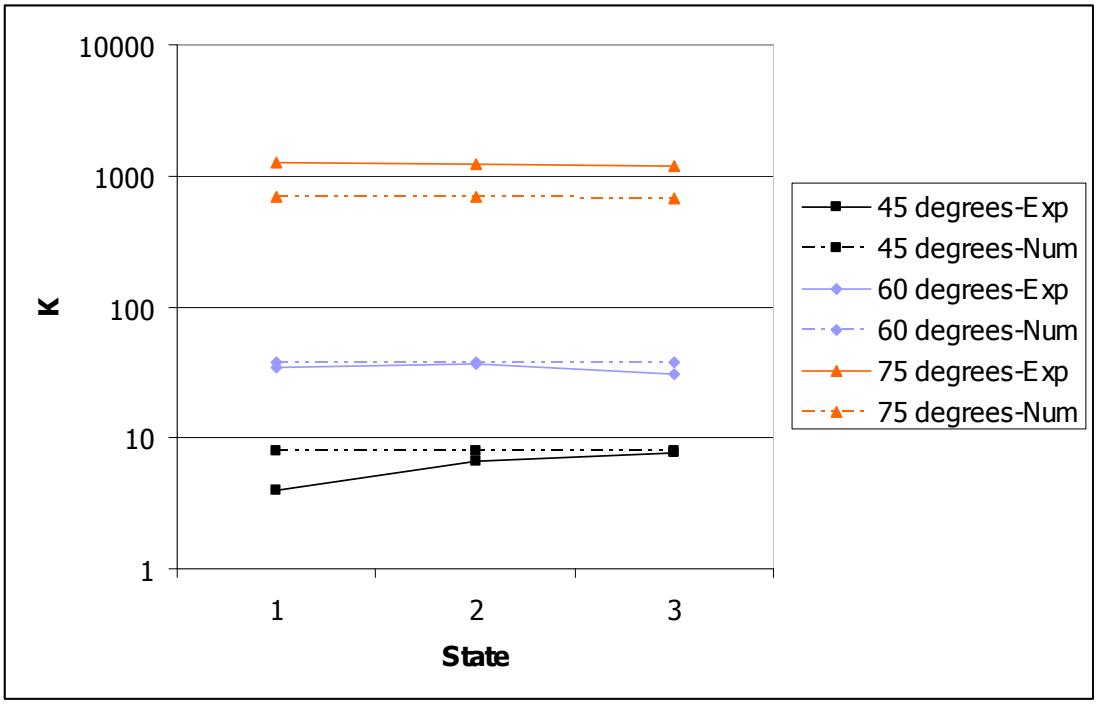

Figure 4.31 : The comparison of the loss coefficient between the experimental and numerical method at 45°, 60° and 75° position under 3 inlet conditions

The torque value was also measured by the experimental and the numerical methods. Fig 4.32 shows the differences between the experimental and numerical results. It was found that results are the closest for the $45°$ position and they become significantly different if the valve angle increases. The closest results are found at $45°$ and $1\,m/s$. It is 14%. However, there are errors in this comparison because the large scale of torque-meter in the experiment.

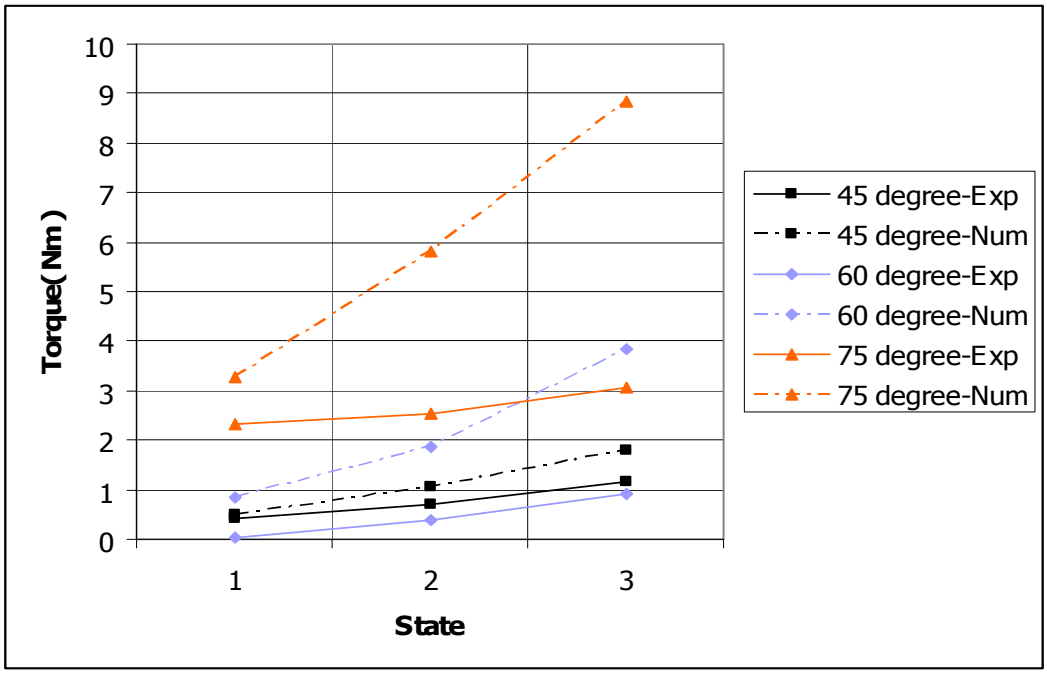

Figure 4.32 : The comparison of the torque characteristic between the experimental and numerical method at $45°$, $60°$ and $75°$ positions under 3 inlet conditions

Chapter 5 Conclusion and Discussion

The investigation of the flow through a butterfly valve was done in both numerical and experimental method to reach the characteristic of loss coefficient and torque behavior. The numerical simulation was done in static and dynamic analysis in 2 different valve sizes, 150 and 300 mm in diameter using commercial fluid dynamics software FLUENT. In static analysis, the numerical method was solved at $0°$, $30°$, $45°$, $60°$ and $75°$ position of the disk under 3 inlet conditions corresponding to $1 m/s$, $2 m/s$ and $3 m/s$. It was found that a bubble occurred behind the valve disk at $45°$ and became bigger when the degree of valve position was increased. On the top view of the flow, wakes, caused by the holes of the motor shaft, can be seen; it was observed that there were bigger if the angle was increased. The loss coefficient can be reduced by decreasing a size of these 2 holes. The loss coefficient is directly dependent on the position of the valve. By increasing the angle of the valve disk, the value of loss coefficient increases. When the inlet load was changed, the value of loss coefficient remains constant. So the loss coefficient is a function of the valve shape. When the investigation of torque characteristic for static analysis was done, it was found that torque value of 300 mm valve is greater than 150 mm because the fluid force distributes on the bigger integral area of the butterfly valve. The torque value is bigger if the angle of the valve disk and the value of velocity inlet increase.

In dynamic analysis, the simulation was carried out in 2 different angular velocities of the valve disk, which are $0.039 rad/s$ (normally rotated condition) and $1.57 rad/s$ (rapidly rotated condition). The velocity inlet was set to a value of $1 m/s$. From this investigation, it was found that the maximum value of the torque appears around $70° - 80°$ position of the butterfly valve. The torque value is decreased in the range of $80° - 100°$ position because the force distribution on the valve surface is balanced itself. After that, by unbalancing force on the valve surface, the torque value increases until it reaches a maximum around the $100° - 110°$ position. It was also found that torque characteristic and value of the normally rotated condition are slightly different with the rapidly rotated condition.

The experiment was carried out under 3 load conditions and 3 different positions of the valve disk, consisting of $45°$, $60°$ and $75°$ position in static analysis. It was found that, when the value of velocity inlet is changed, the value of loss coefficient is not constant at the same position of the disk. These may be due to highly turbulent condition of the water flow in the pipe. Some errors occur at $60°$ position. The torque values, measured at this position are lower than the value at $45°$ position. The cause of this error certainly comes from the range of the torque-meter, too huge for this study. When the comparison between the experimental and numerical results was made, it was found that the loss coefficient and torque values at $45°$ and $60°$ position are acceptable. The mass flow-rate obtained from experimental and numerical method is exactly the same. The numerical results show that they are acceptable and realistic. The trend of characteristic of the loss coefficient and torque values can be seen.

Finally, both experimental and numerical results can be improved in the future. By changing the turbulent model, the numerical results will be more accurate.

To have a better description of the physics of the flow past the butterfly valve, the RNG k-ε model can be used. The Reynolds stress model(RSM), which can give the most accuracy results is another interested model even if it will take a long time for calculation. For the experimental part, the torque-meter has to be changed for a smaller range of measurements. The appropriate range of measurements of the device is necessary for any experiments. All of these changes will lead to the more reasonable results.

References

[1] Leutwyler Z. and Dalton C., 2006, “A Computational Study of Torque and Forces Due to Compressible Flow on a Butterfly Valve Disk in Mid-stroke Position”, ASME J. Fluids Eng., 128, pp.1074-1082

[2] Morris M. J. and Dutton J. C., 1989, “Aerodynamic Torque Characteristics of Butterfly Valves in Compressible Flow”, ASME J. Fluids Eng., 111, pp.392-399

[3] Danbon F. and Solliec C., 2000, “Aerodynamic Torque of a Butterfly Valve-Influence of an Elbow on the Time-Mean and Instantaneous Aerodynamic Torque”, ASME J. Fluids Eng., 122, pp.337-344

[4] Solliec C. and Danbon F., 1999, “Aerodynamic Torque Acting on a Butterfly Valve. Comparison and Choice of a Torque Coefficient”, ASME J. Fluids Eng., 121, pp.914-917

[5] Eom K., 1988, ”Performance of Butterfly Valves as a Flow Controller”, ASME J. Fluids Eng., 110, pp.16-19

[6] Huang C. and Kim R. H., 1996, “Three-Dimensional Analysis of Partially Open Butterfly Valve Flows”, ASME J. Fluids Eng., 118, pp.562-568

[7] Morris M. J. and Dutton J. C., 1991, “An Experimental Investigation of Butterfly Valve Performance Downstream of an Elbow”, ASME J. Fluids Eng., 113, pp.81-85

[8] Morris M. J. and Dutton J. C., 1989, “Compressible Flowfield Characteristics of Butterfly Valves”, ASME J. Fluids Eng., 111, pp.400-407

[9] Idel’cik I. E., 1986,”Memento des Pertes de Charge”, Eyrolles, Paris.

[10] Munson B. R., Young D. F. and Okiishi T. H., 2002, “Fundamental of fluid mechanics”, 4th Edition, John Wiley&Sons Inc, USA